



Original article

Synthesis and pharmacological evaluation of novel fused thiophene derivatives as 5-HT_{2A} receptor antagonists: Molecular modeling study

Mohamed M. El-Kerdawy^a, Eman R. El-Bendary^{b,*}, Alaa A.-M. Abdel-Aziz^c, Dalia R. El-wasseef^a, Naglaa I. Abd El-Aziz^a

^a Department of Medicinal Chemistry, Faculty of Pharmacy, University of Mansoura, Mansoura 35516, Egypt

^b Department of Pharmaceutical Chemistry, Faculty of Pharmacy, King Abdulaziz University, Jeddah 21589, Saudi Arabia

^c Department of Pharmaceutical Chemistry, College of Pharmacy, King Saud University, Riyadh 11451, Saudi Arabia

ARTICLE INFO

Article history:

Received 22 November 2008

Received in revised form

6 January 2010

Accepted 9 January 2010

Available online 20 January 2010

Keywords:

Synthesis

5-HT_{2A} receptor

Antagonists

Molecular modeling

Flexible alignment

Pharmacophore prediction

ABSTRACT

Novel derivatives of cyclopentathienopyrimidinediones **6**, pyridothienopyrimidinediones **7**, ethyl cycloheptathiophene-3-carboxylates **10**, ethyl tetrahydrothienopyridine-3-carboxylates **11**, tetrahydrocycloheptathienopyrimidin-4(3H)-ones **12**, tetrahydrotriazolobenzothienopyrimidin-5(4H)-ones **17** and tetrahydro-5H-cycloheptathienopyrimidin-4(3H)-ones **21** have been synthesized and tested for their 5-HT_{2A} antagonist activity. Preliminary pharmacological studies showed that compounds 3-[2-[4-phenylpiperazin-1-yl]ethyl]-6,7-dihydro-5H-cyclopenta[b]thieno[2,3-d]pyrimidine-2,4(1H,3H)-dione **6a** and ethyl 2-[[4-(2-methoxyphenyl)piperazin-1-yl]acetylamino]-4,5,6,7-tetrahydro-6-methylthieno[2,3-c]pyridine-3-carboxylate **11d** were found to be the most active molecules as 5-HT_{2A} antagonists. Molecular modeling and pharmacophore prediction methodology are used to study the structural features required for 5-HT_{2A} antagonist properties of the active compounds compared with nonactive species by means of the molecular mechanic method. The 2-methoxy substituent in the structure of **11d** seems to be necessary for its full antagonistic properties. Optimal placement of basic nitrogen relative to the plane of thiophene core was found to have a profound effect on affinity and biological activity.

© 2010 Elsevier Masson SAS. All rights reserved.

1. Introduction

The discovery of new ligands with affinity for the family of serotonin receptors is an area of active research in Medicinal Chemistry due to their involvement in numerous physiological and pathophysiological processes [1–9]. Serotonin modulates the activity of both central nervous system and peripheral tissues. It was realized that the action of 5-HT is not all mediated by receptors of the same type and various pharmacological classifications have come and gone. Serotonin is a monoamine neurotransmitter. It is found extensively in the gastrointestinal tract of animals, and about 80–90% of the human body's total serotonin is located in the enterochromaffin cells in the gut, where it is used to regulate intestinal movements [10]. The remainder is synthesized in serotonergic neurons in the central nervous system (CNS) where it has various functions, including the regulation of mood, appetite, sleep, muscle contraction, and some cognitive functions including memory and learning. Serotonin functions as a neurotransmitter in

nerve systems of simple as well as complex animals. Serotonin diffuses to serotonin-sensitive neurons, which control the animal's perception of nutrient availability. Serotonergic signaling plays an important role in the modulation of human mood, anger and aggression. Serotonin has broad activities in the brain, and genetic variation in serotonin receptors and the serotonin transporter, which facilitates re-uptake of serotonin into presynapses, have been implicated in neurological diseases. Drugs targeting serotonin-induced pathways are being used in the treatment of many psychiatric disorders. One focus of clinical research is the influence of genetics on serotonin action and metabolism in psychiatric settings. Such studies have revealed that the variation in the promoter region of the serotonin transporter protein accounts for nearly 10% of total variance in anxiety-related personality [11], and the effect of this gene on depression was found to interact with the environment [12]. Levels of serotonin in the brain show association with aggression [13], and a mutation in the gene which codes for the 5-HT_{2A} receptor may double the risk of suicide for those with that genotype [14]. Serotonin also has effects on appetite, sleep and general metabolism. In the blood, the major storage site is platelets, which collect serotonin from plasma. Bleeding causes serotonin release which constricts blood vessels. Serotonin present in the

* Corresponding author. Tel.: +966 02 6423019; fax: +966 02 6423381.

E-mail address: emanelbendary@yahoo.com (E.R. El-Bendary).

blood then stimulates cellular growth to repair liver damage [15]. Currently, the serotonin receptors are divided into seven main classes, 5-HT_{1–7}, in the central and peripheral nervous systems and in the gastrointestinal tract [16]. With particular emphasis on the 5-HT₂ receptor family, the three receptor subtypes, 5-HT_{2A}, 5-HT_{2B} and 5-HT_{2C}, are G-protein coupled receptors (GPCRs) that couple through the Gq and G11 proteins eliciting their second messenger effects through increases in activity of phospholipase C and/or phospholipase A [17–30]. 5-HT_{2A} receptors are broadly distributed in the prefrontal, parietal, and somatosensory cortex, claustrum, pulmonary arterial rings and in platelets [24–30]. Representative 5-HT_{2A} antagonists include ketanserin (**A**) [24–30], the prototype of a large group of structurally related derivatives such as risperidone (**B**) (Fig. 1) [31]. Other 5-HT_{2A} antagonists, belonging to different chemical classes, include the arylpiperazine derivative [32–45]. The structure–activity data for 5-HT_{2A} antagonists suggest that two planar aromatic or heterocyclic ring systems separated by an aliphatic or alicyclic chain, containing basic protonatable nitrogen, seem to constitute a potent 5-HT_{2A} ligand [42–45]. Additional hydrophobic substituent in the heterocyclic ring, as demonstrated by the 4-fluorophenyl group in sertindole and the chlorophenyl ring in clozapine, enhances the antagonistic potency [33,39]. On the other hand the biophore models for 5-HT_{1A} (Fig. 2) which are marked on the buspirone molecular structure showed four points for fitting including aromatic centroid and three nitrogen centers [42–45]. This three-nitrogen model may induce stabilising effect on the ligand–receptor complexes. Recently, a series of isoindolone derivatives as potent and selective 5-HT_{2C} antagonists were reported [46,47]. Additionally an *in silico* screening approach of the corporate database using a 5-HT_{2C} pharmacophore model resulted in the identification of a related structure containing this template. 5-HT_{2C} pharmacophore model (Fig. 3) consists of a positive ionisable group (blue sphere) which is mapped by the basic nitrogen, an H-bond acceptor (red spheres), mapped by the carbonyl oxygen, an aromatic ring (brown sphere) and 3 hydrophobic groups (orange

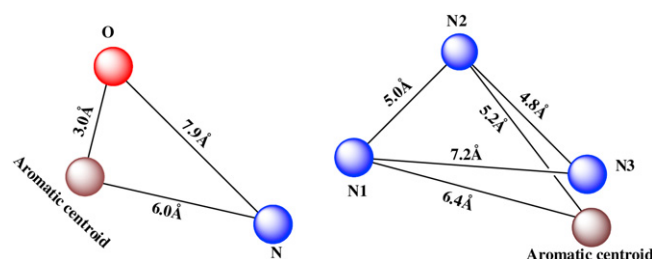


Fig. 2. Proposed pharmacophore models for 5-HT_{2A} (left) and 5-HT_{1A} (right) receptor binding.

spheres) [46,47]. In the course of a program aimed at the discovery of new 5-HT₃ and 5-HT₄ receptor agents, a comparative receptor mapping of both serotonergic binding sites is reported [5,48,49]. This computer-aided conformational analysis has allowed to propose a steric model for 5-HT₃ and 5-HT₄ receptor recognition, which offers structural insights to aid the design of novel selective 5-HT₃ and 5-HT₄ antagonists (Fig. 3) [5,48,49]. This model consists of an aromatic moiety, a coplanar carbonyl group with the oxygen situated at ca. 3.3–3.6 Å from the centroid of the aromatic ring, a nitrogen atom situated at ca. 6.7–8.0 Å from this centroid and ca. 5.2–5.4 Å from the oxygen of the carbonyl group, and a voluminous substituent in the basic amino framework of the molecule (Fig. 3). It was identifying potent and selective 5-HT₆ ligands for cognitive impairment based on novel heterocyclic scaffolds and pharmacophore model shown in Fig. 4 [50]. The basis of this hypothesis is that the basic amine and arylsulfonyl moieties of 5-HT₆ ligands are the necessary receptor pharmacophores and the indole and other heterocyclic cores serve merely as a template to hold these pharmacophores in the necessary orientation (Fig. 4) [50]. The pharmacophore model for 5-HT₇ antagonism was recently described representing the first contribution to the rational design of agents acting at this recently identified serotonin receptor (Fig. 4) [51]. The

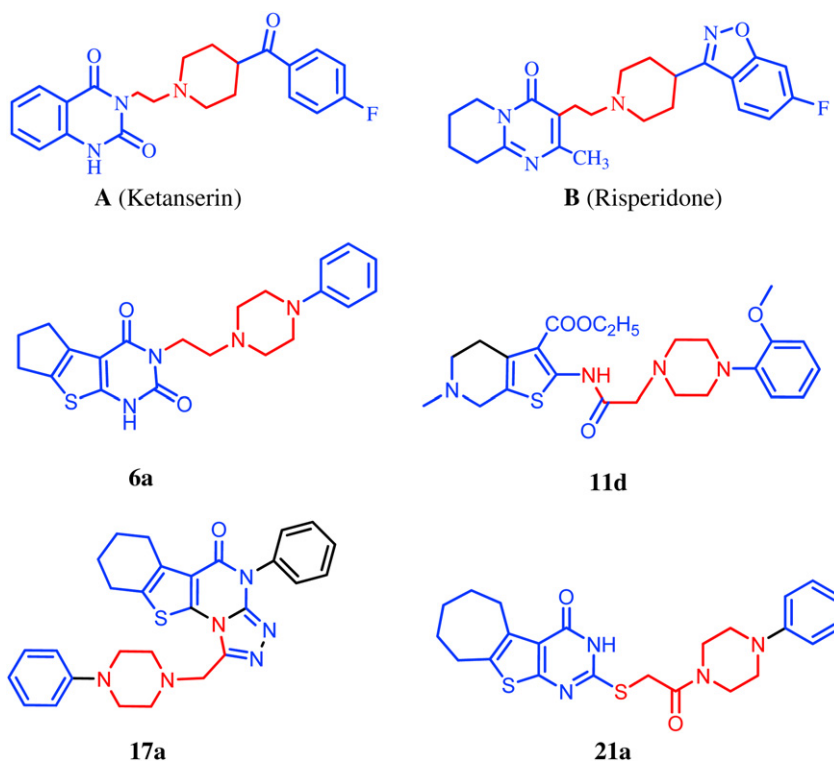


Fig. 1. The reported and the proposed 5-HT_{2A} antagonists.

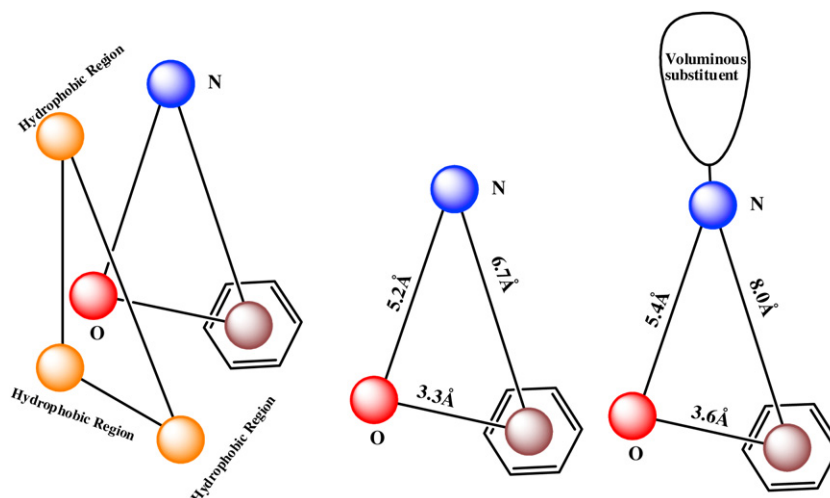


Fig. 3. Proposed pharmacophore models for 5-HT_{2C} (left), 5-HT₃ (middle) and 5-HT₄ (right) receptor antagonists.

postulated hypothesis was validated with a series of new naphtholactam and naphthosultam derivatives that exhibit affinity for the 5-HT₇ receptor. This study offers structural insight to aid the development of novel 5-HT₇ ligands, which are essential for the knowledge of the (patho) physiological role of this serotonin receptor subtype [51].

According to the previous rational, it is reported here the synthesis of some new fused thiophene derivatives and their 5-HT_{2A} antagonistic activity using isolated pulmonary arterial rings of rats [25–30]. These novel synthesized compounds were designed as structurally related to ketanserin A and its analogues risperidone B. Flexible alignment and pharmacophore prediction methodology was used to identify the structural features required for 5-HT_{2A} antagonist properties.

2. Results and discussion

2.1. Chemistry

2.1.1. Synthesis of compounds 1–12 (Scheme 1)

Heterocyclic *o*-amino esters have attracted much attention from the synthetic point of view as they facilitate the preparation of numerous fused heterocyclic systems [52–54]. When an appropriate

cycloalkanone reacted with ethyl cyanoacetate and sulphur in absolute ethanol in the presence of diethylamine they afforded the key starting materials, ethyl 2-amino-5,6-dihydro-4*H*-cyclopenta[*b*]thiophene-3-carboxylate **1**, ethyl 2-amino-5,6,7,8-tetrahydro-4*H*-cyclohepta[*b*]thiophene-3-carboxylate **2**, ethyl 2-amino-4,5,6,7-tetrahydro-6-methylthieno[2,3-*c*]pyridine-3-carboxylate **3** and 2-amino-4,5,6,7-tetrahydrobenzo[*b*]thiophene-3-carboxylate **13** (Schemes 1 and 2).

Reaction of the *o*-amino esters **1** or **3** with 2-chloroethyl isocyanate in toluene afforded the corresponding chloroethyl ureido derivatives **4** and **5** respectively. The structure of the latter compounds was established on the basis of its elemental analysis and spectral data. For example, the ¹H NMR spectrum of compound **4** showed a typical quartet–triplet pattern for the ethyl ester; the triplet appeared at 1.20–1.40 ppm while the quartet was observed at 4.20–4.35 ppm and a multiplet signal of (CH₂CH₂Cl) at 3.60–3.72 ppm. Heating a mixture of the chloroethyl ureido derivatives **4** or **5** and the appropriate *N*-substituted phenylpiperazines at 140 °C afforded 3-[2-[4-substituted phenylpiperazin-1-yl]ethyl]-6,7-dihydro-5*H*-cyclopenta[*b*]thieno[2,3-*d*]pyrimidine-2,4(1*H*,3*H*)-diones **6a–d** and 3-[2-[4-substituted phenylpiperazin-1-yl]ethyl]-5,6,7,8-tetrahydro-7-methylpyrido[4',3':4,5]thieno[2,3-*d*]pyrimidine-2,4(1*H*,3*H*)-diones **7a–d** (Scheme 1). The structures of the isolated products were

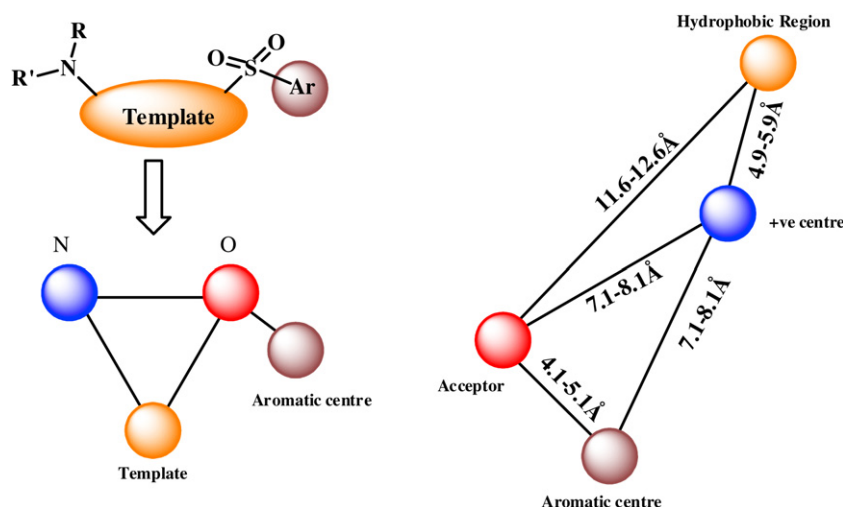
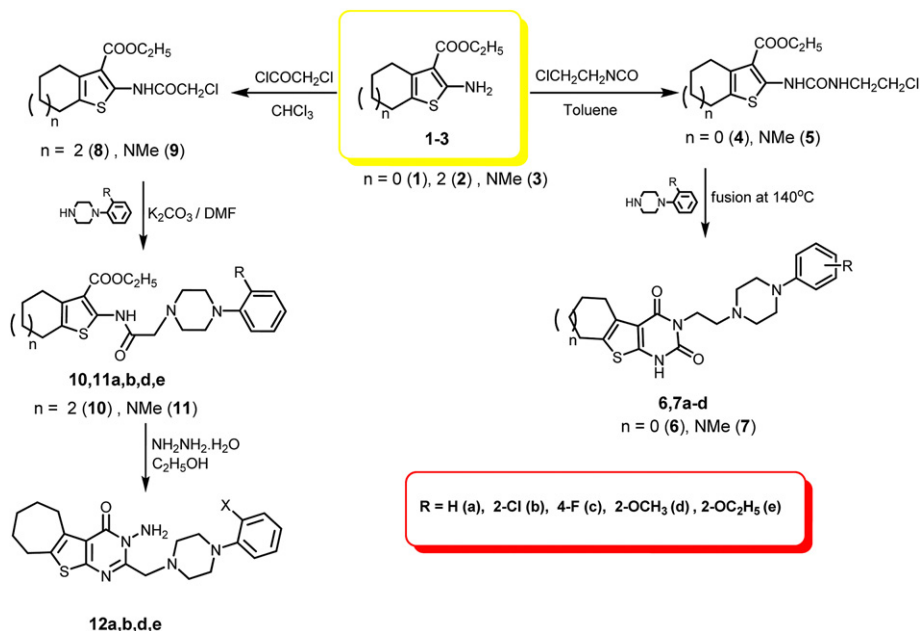


Fig. 4. Proposed pharmacophore models for 5-HT₆ (left) and 5-HT₇ (right) receptor antagonists.

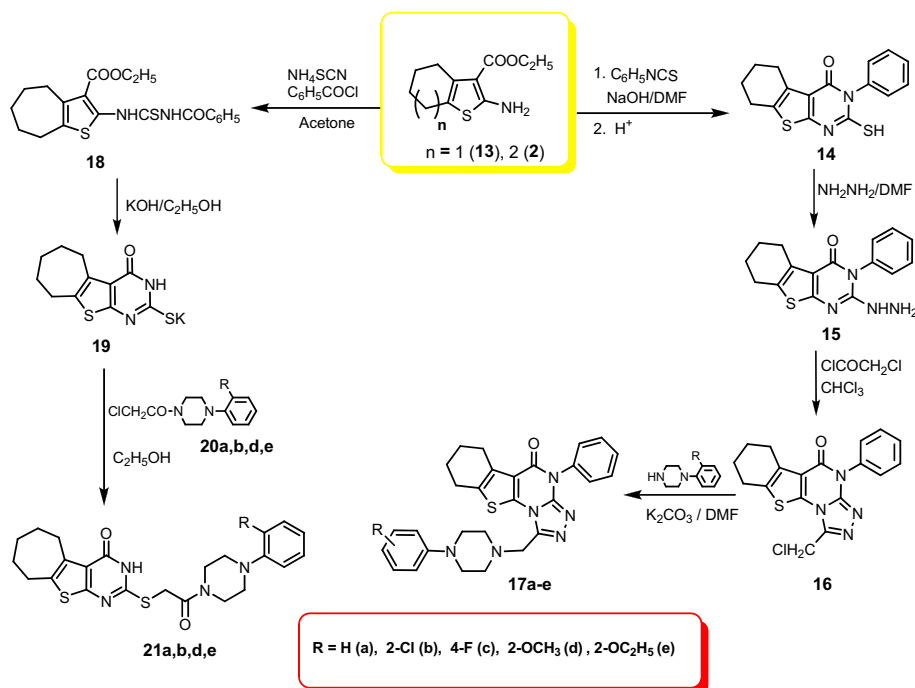


Scheme 1.

established on the basis of their elemental and spectral analyses. For example, the ^1H NMR spectrum showed the disappearance of the signal of the ethyl ester group and the appearance of the protons of the *N*-phenylpiperazine moiety in the expected regions of the spectrum. Condensation of ethyl 2-amino-5,6,7,8-tetrahydro-4*H*-cyclohepta[*b*]thiophene-3-carboxylate **2** or ethyl 2-amino-4,5,6,7-tetrahydro-6-methylthieno[2,3-*c*]pyridine-3-carboxylate **3** with chloroacetyl chloride in chloroform afforded the corresponding chloroacetyl derivatives **8** and **9** respectively. Treatment of the compounds **8** and **9** with the appropriate *N*-substituted phenylpiperazines in the presence of potassium carbonate in DMF afforded ethyl 2-[[4-substituted phenylpiperazin-1-yl]acetyl]amino]-5,6,7,8-

tetrahydro-4*H*-cyclohepta[*b*]thiophene-3-carboxylates **10a,b,d,e** and ethyl 2-[[4-(substituted phenyl)piperazin-1-yl]acetyl]amino]-4,5,6,7-tetrahydro-6-methylthieno[2,3-*c*]pyridine-3-carboxylates **11a,b,d,e** respectively.

Cyclization of compounds **10a,b,d,e** was carried out *via* the reaction with hydrazine hydrate in absolute ethanol to give 3-amino-2-[[4-(substituted phenyl)piperazin-1-yl]methyl]-6,7,8,9-tetrahydro-5*H*-cyclohepta[*b*]thieno[2,3-*d*]pyrimidin-4(3*H*)-ones **12a,b,d,e**. The IR spectrum of compound **12e** revealed the NH₂ and C=O stretching absorption bands at 3280 and 1632 cm⁻¹ respectively. Moreover, the disappearance of the quartet–triplet pattern of the ethyl ester in the ^1H NMR spectrum and the presence of a broad



Scheme 2.

singlet peak at 6.30–6.39 ppm representing (NH₂) group which is a D₂O exchangeable revealed its cyclized structure.

2.1.2. Synthesis of compounds **14–21** (Scheme 2)

Treatment of ethyl 2-amino-4,5,6,7-tetrahydrobenzo[b]thiophene-3-carboxylate **13** with phenyl isothiocyanate in DMF in the presence of sodium hydroxide followed by acidification with dilute acetic acid afforded the mercapto derivative **14**. Compound **14** reacted with hydrazine hydrate in DMF to give the corresponding hydrazino derivative **15** that condensed with chloroacetyl chloride in chloroform to yield the cyclized 1-chloromethyl-4-phenyl-6,7,8,9-tetrahydro[1,2,4]triazolo[4,3-*a*]benzo[b]thieno[3,2-*e*]pyrimidin-5(4*H*)-one **16**. The structure of the latter compound was established on the basis of its elemental analysis and spectral data, for example, the notable feature in the ¹H NMR spectrum being the presence of a singlet peak at 4.65 ppm indicating (CH₂Cl) group. Moreover, a molecular ion peak of *m/z* 371 (5.63%) was clearly identified in the mass spectrum. Compound **16** was treated with the appropriate *N*-substituted phenylpiperazines in DMF to give the corresponding 4-phenyl-1-[[4-substituted phenylpiperazin-1-yl]methyl]-6,7,8,9-tetrahydro-[1,2,4]triazolo[4,3-*a*]benzo[b]thieno[3,2-*e*]pyrimidin-5(4*H*)-ones **17a–e**. The ¹H NMR spectrum of the isolated products **17a–e** showed the appearance of the protons of the *N*-phenylpiperazine moiety in the expected regions of the spectrum.

On the other hand, benzoyl chloride was allowed to react with ammonium thiocyanate in anhydrous acetone at reflux for 10 min, then a solution of ethyl 2-amino-5,6,7,8-tetrahydro-4*H*-cyclohepta[b]thiophene-3-carboxylate **2** in anhydrous acetone was added and the reaction mixture was heated for another 10 min to yield benzoylthioureido derivative **18** in 70% yield. The structure of the latter compound was established on the basis of its elemental analysis and spectral data. For example, the ¹H NMR spectrum showed two broad signals, one at δ 9.00–9.10 and the other appeared at δ 14.50–14.60 representing the two NH groups. Cyclization of the benzoylthioureido derivative **18** in ethanolic potassium hydroxide afforded the potassium salt of 2-mercapto-6,7,8,9-tetrahydro-5*H*-cyclohepta[b]thieno[2,3-*d*]pyrimidin-4(3*H*)-one **19**. The protons of the phenyl ring and ethyl ester in compound **18** disappeared in the ¹H NMR spectrum of compound **19** revealing its cyclization. 1-Chloroacetyl-4-(substituted phenyl)piperazines **20a,b,d,e** were treated with compound **19** to yield 2-[[4-substituted phenylpiperazin-1-yl]carbonylmethylthio]-6,7,8,9-tetrahydro-5*H*-cyclohepta[b]thieno[2,3-*d*]pyrimidin-4(3*H*)-ones **21a,b,d,e**. The structure of the latter compounds was established on the basis of the elemental analyses and spectral data. For example, the ¹H NMR spectrum showed the appearance of the protons of the *N*-phenylpiperazine moiety in the expected regions of the spectrum.

2.2. Biological activity

2.2.1. 5-HT_{2A} antagonist activity using isolated pulmonary arterial rings of rats

Selected examples of the newly synthesized compounds were subjected to an *in vitro* pharmacological screening for 5-HT_{2A} antagonist activities using isolated pulmonary arterial rings of rats [25–30]. Risperidone was chosen as the standard drug. Some of the test compounds in this study inhibited the pressor response of the isolated pulmonary arterial rings to 5-HT (Table 1) and hence showed antagonistic activities for 5-HT_{2A} receptors.

2.2.2. Structure–activity relationship and influence of lipophilic and steric factors

2.2.2.1. Structure–activity relationship. Compound **6a** with a phenylpiperazine moiety joined by an ethylene side chain to a cyclopentathienopyrimidine skeleton exhibited high 5-HT_{2A} antagonist activities. Replacement of the cyclopentyl moiety by a pyridine moiety showed a little effect on decreasing the activities as in compounds **7a**, **7c** and **7d**. Moreover, changing the position of the arylpiperazine moiety to 2 position of pyrimidine ring caused a little decrease in activity such as compounds **21a,b,d**. The higher 5-HT_{2A} antagonist activity of the 2-methoxy derivative **11d** may confirm the importance of this group in the aromatic ring of this skeleton for the activity. The presence of a triazolo moiety between the condensed thienopyrimidine nucleus and the (un)substituted phenylpiperazine moiety greatly decreased the activity which may explain the inactivation of compounds **17a**, **17b** and **17d**. This indicated that the optimal structure for 5-HT_{2A} antagonist is the presence of not more than three fused ring system.

2.2.2.2. Influence of lipophilic and steric factors [39,55]. The introduction of spacer linear alkylic chains of increasing number of carbons between the fused heterocyclic core and arylpiperazine fragment of the new ligands, cycloalkane fragments fused to thiophene moiety and the variation of the substituents on the arylpiperazine fragment [5,6,35,40,41] have allowed evaluating the influence of lipophilicity and steric parameters at the pharmacophoric part of the molecules. Table 1 gathers antagonist activities at 5-HT_{2A} receptors as well as values of log *P* (lipophilic factors) and molar refractometry (steric factors), determined by using HyperChem program [56] for each compound. Within the series of compounds **7a–d** (*n* = NMe) we have observed little increase of the 5-HT_{2A} antagonist activities when molar refractometry increases from 121.2 cm³/mol (*R* = H) to 128.4 cm³/mol (*R* = OMe). Such phenomenon was observed within other series such as compounds **6a** and **11d** with molar refractometry values 112.3 cm³/mol and 133.8 cm³/mol respectively. Although lipophilicity does not exert a significant effect on affinity for compounds **7a–d**, **6a** and **11d**,

Table 1

Response % of the tested compounds (mmol/kg) towards inhibition of 5-HT induced pulmonary arterial ring pressor and molecular parameters of some selected compounds.

Compd. no.	Response ^a [%]	Log <i>P</i> ^b	MR ^c [cm ³ /mol]	Compd. no.	Response ^a [%]	Log <i>P</i> ^b	MR ^c [cm ³ /mol]
6a	86	1.5	112.3	12d	66	2.1	127.6
7a	60	0.7	121.2	17a	0	4.9	145.7
7c	63	0.9	121.6	17b	0	5.5	150.3
7d	65	0.5	128.4	17d	0	4.7	153.0
11a	62	0.8	126.5	21a	65	2.6	127.8
11d	88	0.6	133.8	21b	60	3.1	132.4
11e	65	0.9	138.6	21d	68	2.4	135.0
				Risperidone	100	2.7	114.2

^a Response % of the tested compounds (mmol/kg) towards inhibition of 5-HT induced pulmonary arterial ring pressor.

^b Calculated lipophilicity.

^c Molar refractometry.

a remarkable decrease in potency was observed for **17a–d**, with values of $\log P$ higher than 4.7. Moreover, a spacer carbon chain with one carbon atom between the arylpiperazine and heterocyclic core diminishes the activity as in compound **17**, if compared with compounds **6**, **7**, **11**, **12**, and **21**. Variations of lipophilicity produced by cycloalkanone ($n = 0, 2$, NMe) or aromatic substituents ($R = H$, Cl and OMe) did not notably alter 5-HT_{2A} antagonist activities. Similarly, for analogues **21a–d** no significant variations in 5-HT_{2A} antagonist activity were found, pointing out that lipophilicity of the molecules is not a crucial factor for the activity. Regarding steric parameters, from the data gathered in Table 1 there is a clear influence of refractometry on 5-HT_{2A} antagonist activity compared with lipophilicity for either series of all compounds. The optimal lipophilicity and steric parameters for the active compounds was in range of 0.5–3.1 and 112.3–138.6 cm³/mol, respectively, higher values diminished the activity.

2.3. Molecular modeling study

Modeling studies are required in order to construct molecular models that incorporate all experimental evidence reported. These models are necessary to obtain a consistent, more precise picture of the biologically active molecules at the atomic level and furthermore, provide new insights that can be used to design novel therapeutic agents. Considering ligand–receptor interaction, one usually takes into account two points: strength of the interaction (what we refer to as ‘affinity’) and type of an effect at the biochemical, electrophysiological and behavioural level triggered by the ligand (what we refer to as ‘intrinsic activity’). To get an insight into the type of chemical forces involved in the interaction, one either builds models of a specific pharmacophore or constructs models of a receptor protein and examines the binding forces. Interaction of a ligand with a receptor may result in receptor activation (agonists), blockade (antagonists) or inactivation (inverse agonists) [5,6,49,57,58].

2.3.1. Conformational analysis

An attempt to gain a better insight into the molecular structures of the active compounds **6a**, **11d** and **21d** and inactive compound **17a** as a representative example, conformational analysis of the target compound has been performed by use of the molecular mechanics (MM+) [59,60] force-field (calculations in vacuo, bond dipole option for electrostatics, Polak–Ribiere algorithm and root mean square (RMS) gradient of 0.01 kcal/Å mol) as implemented in HyperChem 5.1 [56]. The most stable conformer was fully optimized with AM1 semi-empirical molecular orbital calculation [61]. The global minimum was confirmed as true minimum, not saddle

point by the absence of negative eigen value of the Hessian through frequency calculation [62–65]. Two main conformers were observed for all compounds under investigation including *extended*- and *folded*-conformers. At this stage, calculations at the AM1 level were considered in order to determine relative energies of the *extended*- and *folded*-conformers of compounds under studies. The results show that *extended*-conformers were more stable than *folded*-conformers by 3–4 kcal/mol (Fig. 5).

2.3.2. Flexible alignment and RMS fit overlay

2.3.2.1. Flexible alignment. Flexible alignment is an application for flexibly aligning small molecules. The method accepts as input a collection of small molecules with 3D coordinates and computes a collection of alignments. Each alignment is given a score that quantifies the quality of the alignment in terms of both internal strain and overlap of molecular features. Often, atomic-level details of the structures of pharmaceutically relevant receptors are not available. In such cases, 3D alignment (or superposition) of putative ligands can be used to deduce structural requirements for biological activity. Methodologies based upon 3D alignment for finding biologically active ligands generally make use of the qualitative assumption that if two ligands have similar biological activity and bind in similar modes, then the bound conformations of the two ligands align well and inferences can be made about the nature of the receptor [66,67].

To probe similarity between the three-dimensional structures of active compounds **6a** and **11d**, flexible alignments were employed. Our initial approach was to employ MOE/flexible alignment [68] to automatically generate superpositions of the compounds under investigation with minimal user bias. Using MOE/MMFF94, 150 conformers of each compound were generated and minimized with a distance-dependent dielectric model. A low energy set of 50 was selected for further analysis. Conformations of compound **6a** were generated using distance geometry and optimized with MMFF94 [69]. Nine low energy, maximally dissimilar structures were selected for comparison to the other compound **11d**. After assigning MMFF94 charges to all molecules, flexible alignment was employed to scan and rank overlays of compounds **6a** and **11d** based on steric, electrostatic field, hydrophobic areas overlap, hydrogen bond donors and acceptors overlap. From the top scoring superposition, several sets most consistent with the structure–activity relationships of the two 5-HT_{2A} antagonist compounds were selected and subjected to more refined searching using MOE/flexible alignment module [68], the highest scoring aligned pair is shown in Fig. 6a. Since both molecules are highly flexible, the limited set of conformers used in the analysis was not capable of achieving

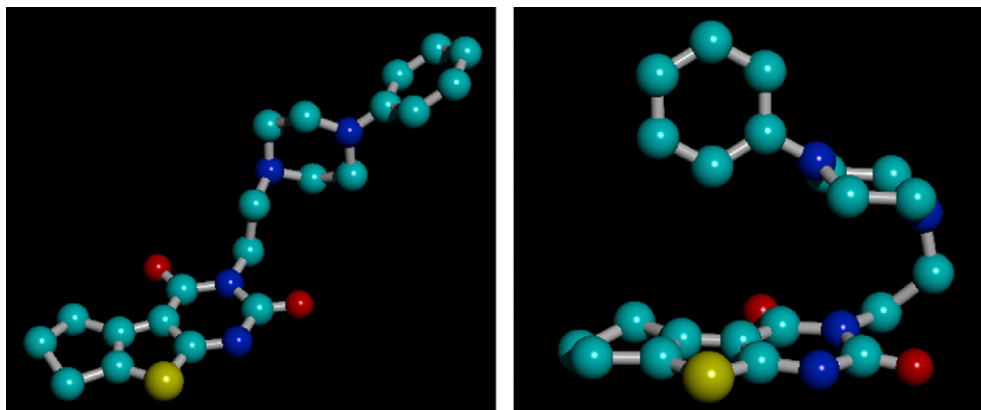


Fig. 5. Energy minimization of compound **6a** as a representative example showing the *extended*-conformer (left panel) and the *folded*-conformer (right panel).

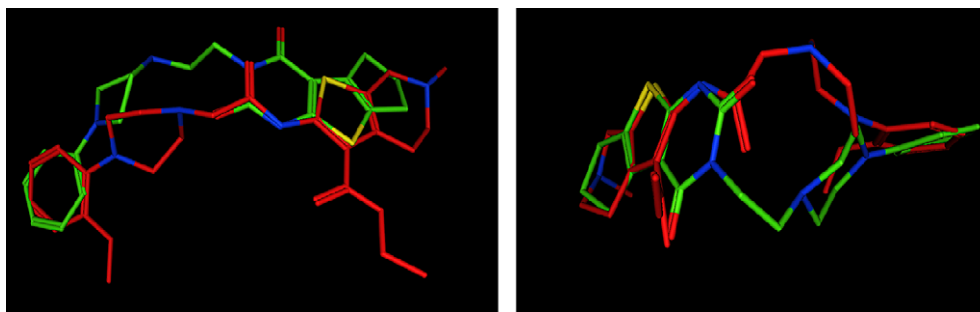


Fig. 6. (a, Left) Superposition of the most active compounds **6a** (in green) and **11d** (in red) using flexible alignments. (b Right) Further refinement of the overlay subjected to the constraints described in the text.

complete atom to atom superposition. A further refinement was generated (Fig. 6b) by constraining the functional group mapping suggested from the initial alignment. The calculated energy difference between the native conformers derived from the flexible alignment (Fig. 6a) and the final conformers in Fig. 6b is minimal. In fact, the refined structure of compound **6a** was 0.5 kcal/mol lower in energy than the starting structure, and compound **11d** was 1.0 kcal/mol lower. A common feature of the MOE-generated alignments is the superposition of the carbonyl group of both compounds. As shown in Fig. 6b, the carbonyl unit of compound **6a** maps to the carbonyl of the compound **11d** (0.8 Å). The aromatic ring and basic nitrogen of piperazine nucleus align fairly well for both compounds and almost complete superposition of the thiophene rings of compounds **6a** and **11d** (0.1 Å).

By the same way, 5-HT_{2A} antagonist compounds **6a**, **11d**, **21a** and inactive compound **17a** were subjected to flexible alignments. As shown in Fig. 7, all active compounds have the same feature of alignment as we described above showing four points of similarities; aromatic thiophene core, carbonyl group directly attached to thiophene moiety, basic nitrogen of piperazine fragment and aromatic ring attached to such basic nitrogen. This alignment suggests the possible existence of a region on the receptor suited for specific recognition of such features. This hypothesis is also supported by the known preference for serotonin receptor recognition [45,51]. Analysis of inactive molecule is an important step to understand the essential features for a given activity. It is clear that compound **17a** was flexibly aligned in a different manner when compared to the active compounds explaining why such compound was void of 5-HT_{2A} antagonist activity (Fig. 7).

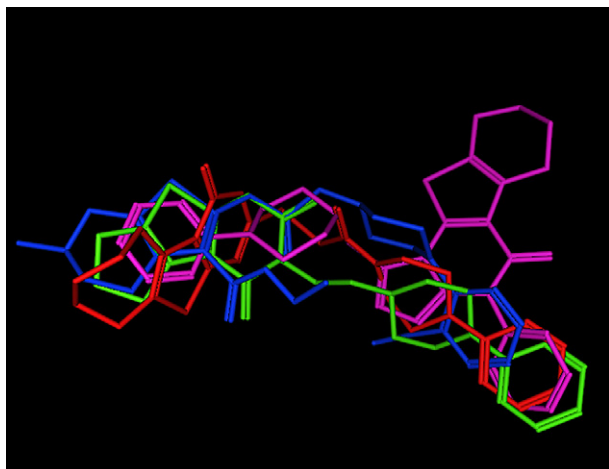


Fig. 7. Flexible alignment of the active compounds **6a** (green), **11d** (blue), **21a** (red) and the inactive compound **17a** (violet).

2.3.2.2. RMS fit overlay (rigid alignment). It is obvious from the flexible alignment, the occurrence of four points of similarities among the active compounds. However, from these results alternative mappings for all compounds under investigation were also identified using rigid overlays methodology. The stable *extended*-conformers resulting from computational chemistry analysis using MM+ force-field [59,60] as implemented in HyperChem 5.1 [56] were superimposed in order to reveal the similarities and differences in structure (Fig. 8). The strategy of overlay fit was to match thiophene rings and to examine any spatial differences between the atoms of the arylpiperazine moieties. As shown in Fig. 8, the carbonyl unit and thiophene core of all compounds completely align (0.1–0.3 Å). The aromatic ring and basic nitrogen of piperazine nucleus for active compounds **6a**, **11d** and **21a** align fairly well (1.2–2.3 Å). More interestingly, the aromatic ring and the basic nitrogen of the inactive compound **17a** completely deviated from the active analogues by 9.7 Å and 7.9 Å respectively (Fig. 8). Examination of Fig. 8 reveals that no element of compound **17a** correlates with the 5-HT_{2A} antagonist activity and this is not surprising in the context of the structure–activity relationships.

2.3.3. Electrostatic and hydrophobic mappings

In an attempt to understand the inactivity of compound **17a** and 5-HT_{2A} antagonist activity of **6a**, **11d** and **21a**, electrostatic and hydrophobic mappings have been carried out for the lowest energy conformers, to examine the similarity and dissimilarity in electronic, electrostatic binding characteristics of the surface of the



Fig. 8. RMS fit overlay (rigid alignment) of the active compounds **6a** (green), **11d** (blue), **21a** (red) and the inactive compound **17a** (violet).

molecules and conformational properties (Figs. 9 and 10). Comparison of the electrostatic mappings of **6a**, **11d** and **21a** shows that increased negative charge regions located on the carbonyl groups representing hydrogen bond acceptor regions (in red) and medium polar heterocyclic nitrogen atoms located on the basic nitrogen of piperazine moieties (in cyan). Such results indicated the structural similarity among these analogues and so similar biological activity as evident from the experimental data (Fig. 9). In

contrast, the inactivity of compound **17a** may be attributed to the difference in electrostatic mapping in which the red hydrogen bond acceptor area was located on the heterocyclic triazole ring (Fig. 10).

Similarly, hydrophobic mappings of active compounds showed that the hydrophobic region in green was distributed on both sides of aromatic ring of arylpiperazine moieties and thiophene core while the hydrophilic region in red was located mainly on carbonyl groups. On the other hand the hydrophobic distributions of the

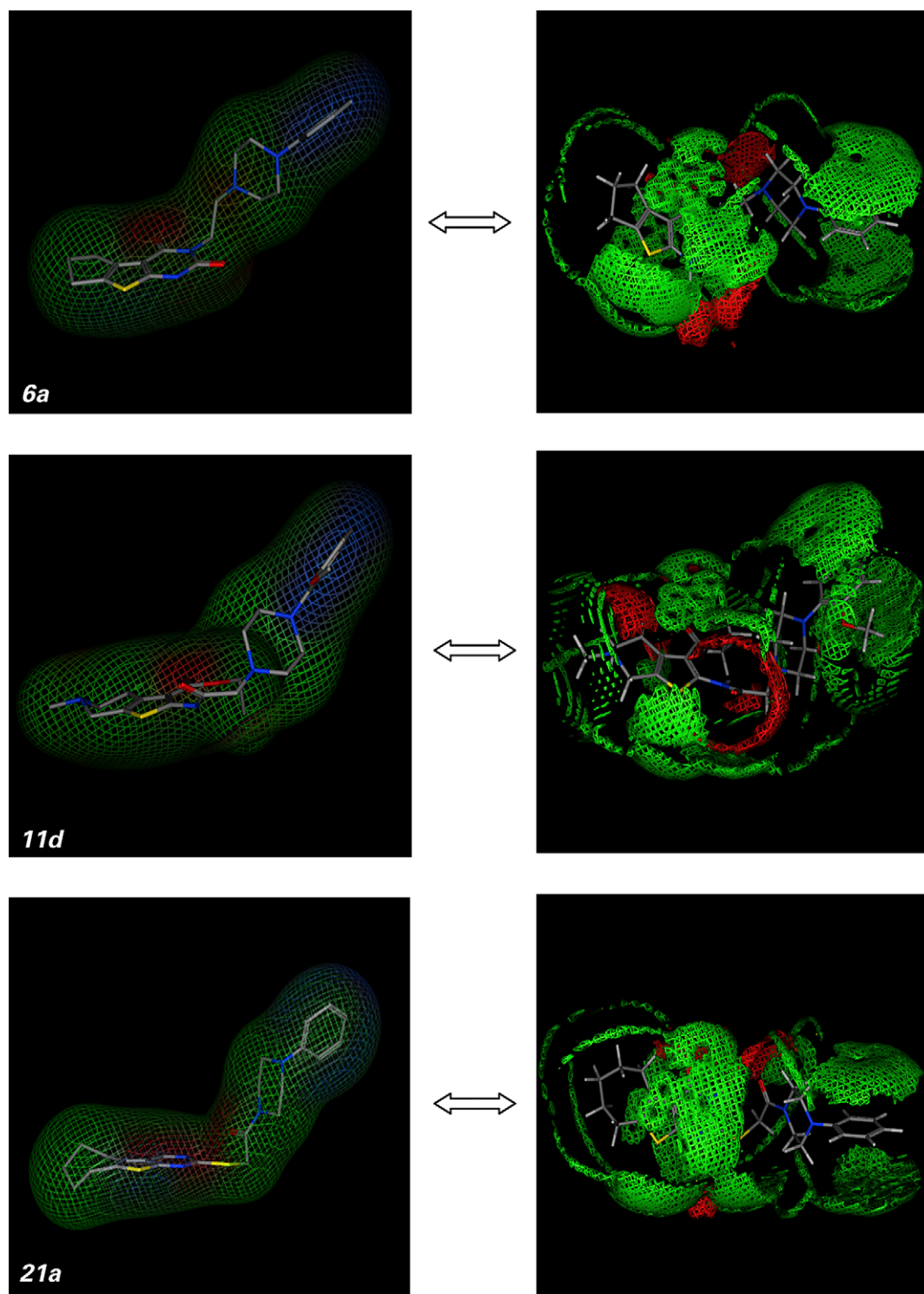


Fig. 9. Electrostatic maps (left panels) and hydrophobic maps (right panels) of the lowest energy conformers for the active compounds **6a**, **11d** and **21a**, maps are color coded: red for a hydrogen bond and a hydrophilic region, cyan for a medium polar region, and green for a hydrophobic region.

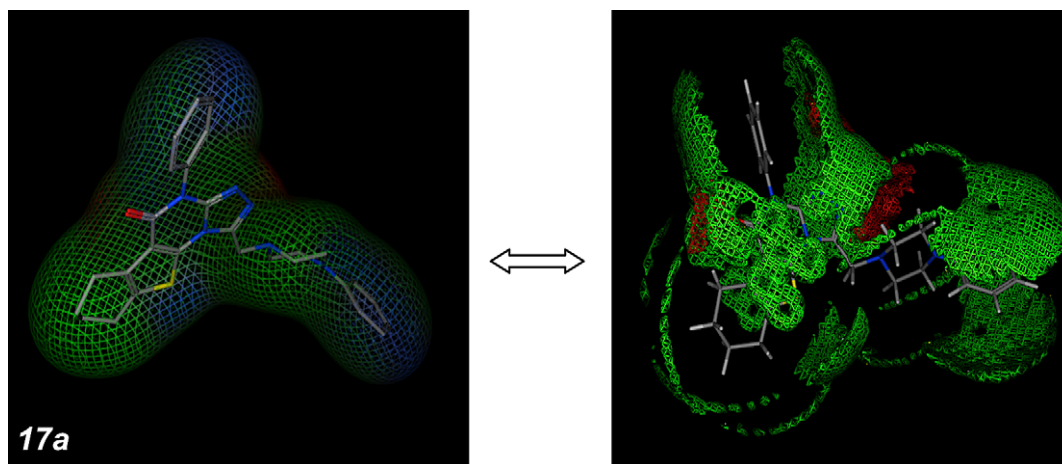
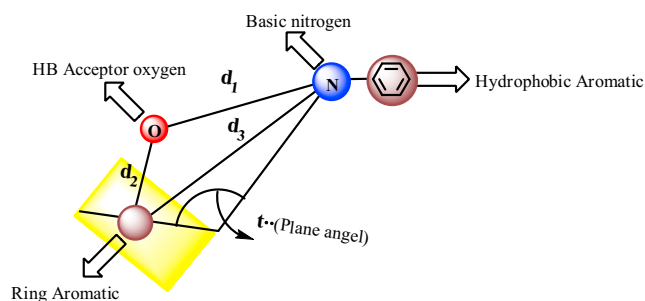


Fig. 10. Electrostatic maps (left panels) and hydrophobic maps (right panels) of the lowest energy conformer for the inactive compound **17a**, maps are color coded: red for a hydrogen bond and a hydrophilic region, cyan for a medium polar region, and green for a hydrophobic region.

inactive compound **17a** occupy an additional aromatic ring indicating the higher lipophilicity of such compound while the hydrophilic red region was located on the triazole ring.

It is clear that the related charge distribution, electrostatic and hydrophobic mappings suggest a similar interaction of the molecules with a potential protein-binding site. As a result, we find that compounds **6a**, **11d** and **21a** all can adopt conformations that have identical distances and orientations of the protein-binding site and that show sufficient agreement of the overall structure and of the electrostatic potential pattern. Consequently these conformations permit approach to a protein surface in much the same way connecting to a binding site that fits all three ligands (Table 2). They can thus be regarded as the active binding conformations. Further reorientation at the site will lead to an induced fit different for the specific ligands and responsible for variations in their binding affinity.

Table 2
Proposed pharmacophore model for 5-HT_{2A} receptor antagonists and structural parameters of the lowest energy extended-conformers of analyzed compounds.



Compd.	d_1^a (Å)	d_2^b (Å)	d_3^c (Å)	Plane angle ^d (°)
6a	7.0	3.5	8.8	142.4
11d	6.6	3.4	7.4	152.9
17a	10.3	3.1	8.2	123.3
21a	7.2	3.8	8.2	141.0

^a Distance between the basic nitrogen and the oxygen of the carbonyl group.

^b Distance between the centroid of the ring aromatic and the oxygen of the carbonyl group.

^c Distance between the basic nitrogen and the centroid of the hydrophobic aromatic.

^d Angle between the basic nitrogen and the plane of the ring aromatic.

2.3.4. Pharmacophore prediction [45,51,70]

For pharmacophore generation and prediction, compound **11d** (Fig. 11) served as the reference to which all conformations of each analogue were aligned. All structures were built de novo using 2D/3D editor sketcher in MOE [68]. Conformational models were calculated using a 15 kcal energy cut off (minimization convergence criteria during conformational analysis: energy convergence = 0.01 kcal/mol, gradient convergence = 0.01 kcal/mol). The number of conformers generated for each substrate was limited to a maximum of 150. All molecules with their associated conformations were regrouped including the biological data. Hypothesis generation was performed using low energy conformers of the molecules. After assignment of possible pharmacophore elements for each analogue the calculation and analysis were carried out using the MOE program [68] and a superposition of the molecules, including the assigned elements, was attempted (Figs. 11 and 12). Several runs of calculation were repeated to generate pharmacophore maps. For each run a distinct number of specified pharmacophore elements were adapted. All adapted models showed that the acceptor atoms of the carbonyl and basic nitrogen fragments as hydrophilic element and the aromatic rings as hydrophobic element were well superimposed within the set distance tolerance. This confirms the important role of the hydrophilic and hydrophobic moieties for recognition and binding to receptor sites.

Models for **11d** and its analogues **6a** and **21a** (Fig. 11, Table 2) possess pharmacophore elements in the piperazine basic nitrogen which is out of the thiophene plane as well as carbonyl moiety in the same plane of thiophene core. In contrast, model for **17a** (Fig. 12, Table 2) showed common elements only in carbonyl oxygen and thiophene core fused to non-favourable triazole fragment. Since the arylpiperazine part of compound **11d** plays an important role in binding, model **17a** was excluded from further considerations. Therefore, model **11d** was considered as the representative pharmacophore map of the antagonism fitting the binding site.

According to the pharmacophore generated by MOE [68] and DSV [71], the minimal structural requirements for 5-HT_{2A} antagonism consist of an aromatic ring, a basic nitrogen atom, an H-bonding acceptor group and a hydrophobic region directly attached to the basic center (Table 2). For all the active molecules, reasonable nonbonded distances among the basic nitrogen, carbonyl group and the thiophene centroid as well as bond angles between the plane of the thiophene core and the basic nitrogen aligned on the

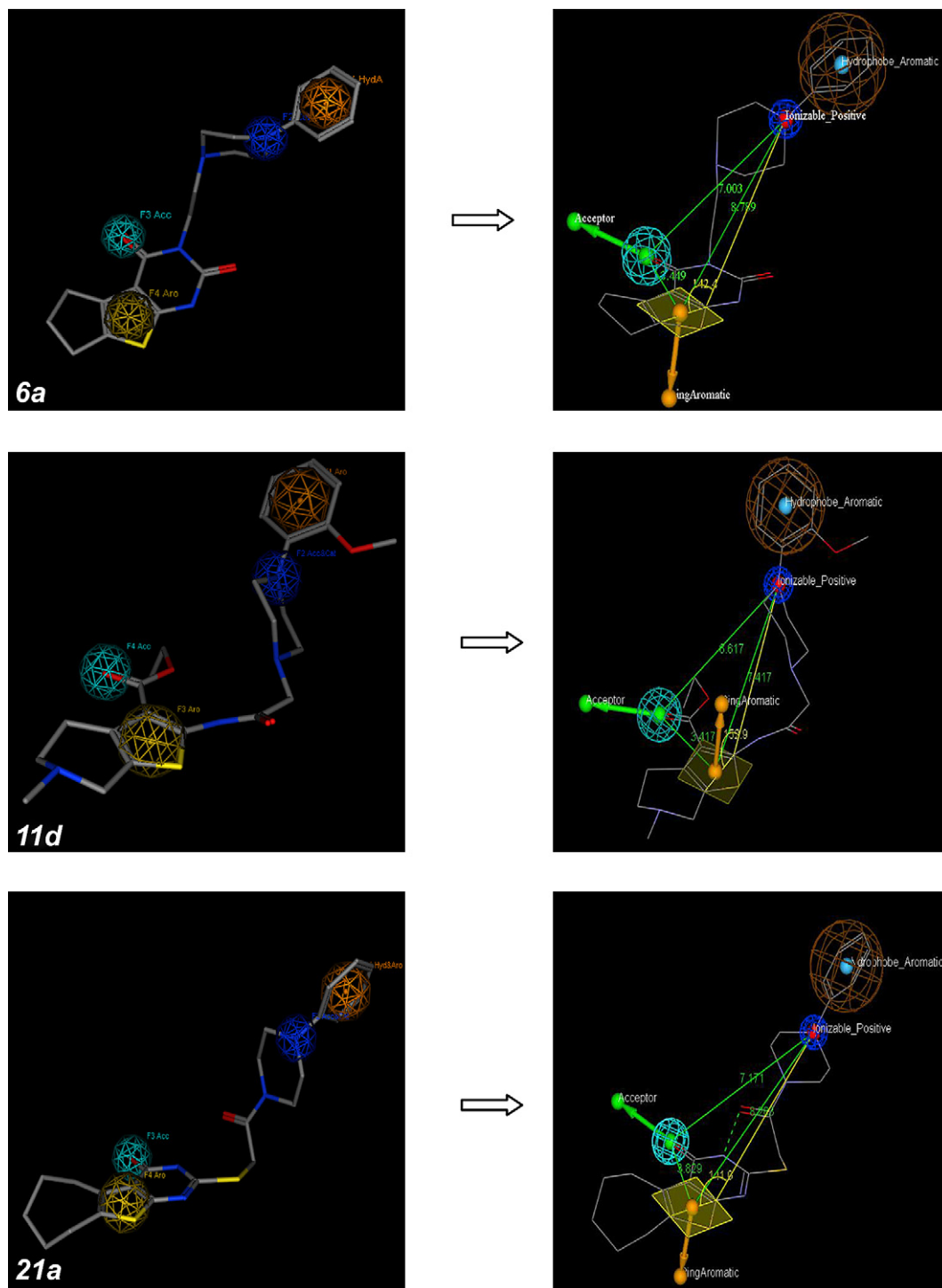


Fig. 11. The active compounds **6a**, **11d** and **21a**, mapped to the pharmacophore model for 5-HT_{2A} receptor antagonists. Pharmacophore features are color coded: brown and yellow for hydrophobics aromatic, cyan for a hydrogen bond acceptor, and blue for a positive ionisable feature.

predicted pharmacophore maps were found (Table 2). This pharmacophoric assumption was in consistency with reported results for 5-HT_{2A} antagonist activity [39–41,45,49,51,57,59].

3. Conclusion

The present work led to the development of novel 5-HT_{2A} antagonist molecules and two of the novel agents namely, 3-[2-[4-phenylpiperazin-1-yl]ethyl]-6,7-dihydro-5H-cyclopenta[b]thieno-

[2,3-d]pyrimidine-2,4(1H,3H)-dione **6a** and ethyl 2-[[4-(2-methoxyphenyl)piperazin-1-yl]acetylaminol]-4,5,6,7-tetrahydro-6-methylthieno[2,3-c]pyridine-3-carboxylate **11d**, which have shown higher antiserotonergic activities than all the other tested compounds.

Flexible alignment was conducted on the basis of experimental data from which four featured pharmacophore model was developed. The model was mapped onto the 5-HT_{2A} antagonist molecules and compared with nonactive compounds. This model justifies the importance of the main pharmacophore groups

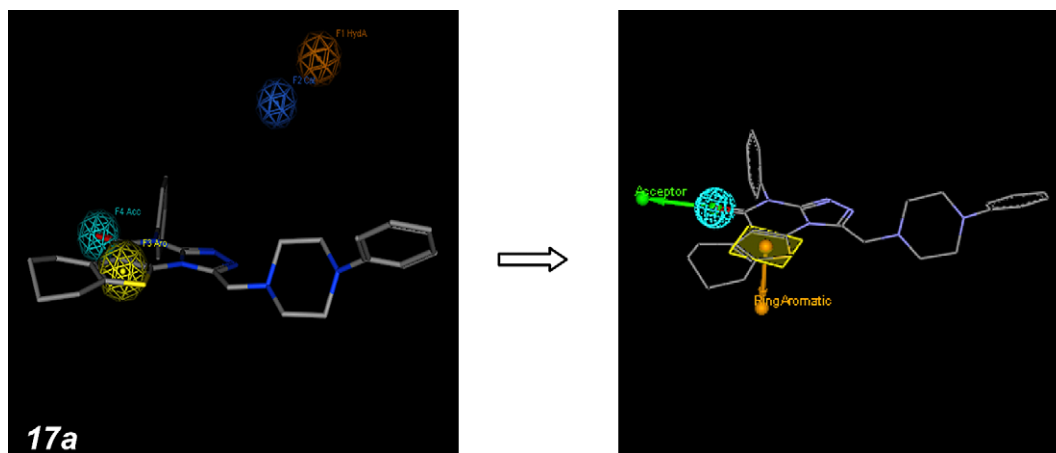


Fig. 12. The inactive compound **17a**, mapped to the pharmacophore model for 5-HT_{2A} receptor antagonists. Pharmacophore features are color coded: brown and yellow for hydrophobic aromatics, cyan for a hydrogen bond acceptor, and blue for a positive ionisable feature.

(particularly, the carbonyl fragment and the basic nitrogen atom) as well as of their relative distance. In fact, while the substitution pattern on the phenyl ring considerably affects the activity (with the *o*-methoxy substituent associated with the best activity), spatial considerations are particularly important for the basic nitrogen atom, since its spatial locations in regard to the plane of thiophene core are critical for the biological activity. Therefore, our pharmacophore model could be very useful for the virtual screening in the development of new 5-HT_{2A} antagonists.

4. Experimental

4.1. General

Melting points were measured with a *Fisher-Johns* melting point apparatus and are uncorrected. IR spectra were recorded on Mattson 5000 FT-IR spectrometer. ¹H NMR spectra were determined in CDCl₃ or DMSO-*d*₆ on FT-NMR spectrometer (200 MHz) Gemini Varian using TMS as internal standard. Mass spectra were measured on JEOL JMS-600H spectrometer. Elemental analysis was carried out at the Microanalytical Center of Cairo University. *o*-Amino esters **1–3**, **13** [52–54], ethyl 2-[(chloroacetyl)amino]-5,6,7,8-tetrahydro-4*H*-cyclohepta[*b*]thiophene-3-carboxylate **8** [54], 2-mercapto-3-phenyl-5,6,7,8-tetrahydrobenzo[*b*]thieno[2,3-*d*]pyrimidin-4(3*H*)-one **14** [72,73], 2-hydrazino-3-phenyl-5,6,7,8-tetrahydrobenzo[*b*]thieno[2,3-*d*]pyrimidin-4(3*H*)-one **15** [74] and 1-chloroacetyl-4-substituted phenylpiperazines **20** [75–77] were prepared following the procedures reported in the literature.

4.2. Ethyl 2-[3-(2-chloroethyl)ureido]-3-carboxylates **4,5** (Scheme 1)

2-Chloroethyl isocyanate (1.58 g, 15 mmol) was added to a suspension of **1** or **3** (10 mmol) in hot toluene (20 ml) and the reaction mixture was heated under reflux for 6 h. The solvent was then evaporated under reduced pressure. The residue of compound **4** was chromatographed on silica gel and eluted with ethyl acetate:petroleum ether (1:4) to give the ureido derivative **4**. The residue of compound **5** was triturated with a little amount of ethanol and the separated solid was filtered, dried and crystallized from water.

4.2.1. Ethyl 2-[3-(2-chloroethyl)ureido]-5,6-dihydro-4*H*-cyclopenta[*b*]thiophene-3-carboxylate **4**

White shiny needles (1.26 g, 40%) mp 118–119 °C. IR (KBr) ν_{max} /cm⁻¹ 3220, 3145 (NH), 1740 (COOC₂H₅), 1640 (C=O). ¹H NMR (CDCl₃); δ 1.20–1.40 (t, 3H, OCH₂CH₃), 2.25–2.43 (m, 2H, CH₂), 2.70–

2.90 (m, 4H, 2CH₂), 3.60–3.72 (m, 4H, CH₂CH₂Cl), 4.20–4.35 (q, 2H, OCH₂CH₃), 5.50–5.70 (br s, 1H, NH, D₂O exchange.), 10.25–10.30 (br s, 1H, NH, D₂O exchange.). Anal. Calcd. for C₁₃H₁₇ClN₂O₃S: C, 49.29; H, 5.41; N, 8.84. Found: C, 49.60; H, 5.38; N, 9.25.

4.2.2. Ethyl 2-[3-(2-chloroethyl)ureido]-4,5,6,7-tetrahydro-6-methylthieno[2,3-*c*]pyridine-3-carboxylate **5**

Brown powder (2.07 g, 60%) m.p. 219–220 °C. ¹H NMR (DMSO-*d*₆); δ 1.30–1.40 (t, 3H, OCH₂CH₃), 2.70–3.00 (m, 7H, 2CH₂, NCH₃), 3.40 (s, 2H, CH₂), 3.60–3.80 (m, 4H, CH₂CH₂Cl), 4.50–4.60 (q, 2H, OCH₂CH₃), 6.30 (s, 1H, NH, D₂O exchange.), 10.30–10.50 (br s, 1H, NH, D₂O exchange.). MS *m/z* (%) 347 (M⁺ + 1, 20.99), 346 (M⁺, 30.09), 308 (18.51), 240 (15.84), 239 (64.16), 125 (100), 122 (17.53). Anal. Calcd. for C₁₄H₂₀ClN₃O₃S: C, 48.62; H, 5.83; N, 12.15. Found: C, 48.94; H, 5.45; N, 12.48.

4.3. 3-[2-[4-Substituted phenylpiperazin-1-yl]ethyl]-6,7-dihydro-5*H*-cyclopenta[*b*]thieno[2,3-*d*]pyrimidine-2,4-(1*H*,3*H*)-diones and 3-[2-[4-substituted phenylpiperazin-1-yl]ethyl]-5,6,7,8-tetrahydro-7-methylpyrido[4',3':4,5]thieno[2,3-*d*]pyrimidine-2,4-(1*H*,3*H*)-diones **6,7a–d** (Scheme 1)

A mixture of the ureido derivative **4** or **5** (5 mmol) and the appropriate *N*-substituted phenylpiperazine (25 mmol) was heated in an oil bath for 6–8 h at 140 °C. After cooling, the reaction mixture was treated with a small amount of ethanol and the solid obtained was filtered off. The filtrate was evaporated under reduced pressure and the solid obtained was crystallized from DMF. The sticky product, compound **6b** was chromatographed on silica gel and eluted with ethyl acetate:petroleum ether (1:4).

4.3.1. 3-[2-[4-Phenylpiperazin-1-yl]ethyl]-6,7-dihydro-5*H*-cyclopenta[*b*]thieno[2,3-*d*]pyrimidine-2,4-(1*H*,3*H*)-dione **6a**

Yellow crystal (0.79 g, 40%) m.p. 132–133 °C. IR (KBr) ν_{max} /cm⁻¹ 3210, 3150 (NH) and 1647, 1640 (C=O). MS *m/z* (%); 396 (M⁺, 0.54), 335 (0.57), 207 (0.37), 189 (3.26), 162 (24.74), 120 (100), 56 (22.38). Anal. Calcd. for C₂₁H₂₄N₄O₂S: C, 63.61; H, 6.10; N, 14.13. Found: C, 63.35; H, 6.45; N, 14.54.

4.3.2. 3-[2-[4-(2-Chlorophenyl)piperazin-1-yl]ethyl]-6,7-dihydro-5*H*-cyclopenta[*b*]thieno[2,3-*d*]pyrimidine-2,4-(1*H*,3*H*)-dione **6b**

Yellow powder (0.71 g, 33%) m.p. 120–122 °C. ¹H NMR (CDCl₃); δ 2.30–2.40 (m, 2H, CH₂), 2.80–2.92 (m, 4H, 2CH₂), 3.20–3.80 (m, 12H, 3NCH₂, 2Ar-NCH₂, CONCH₂), 6.90–7.50 (m, 4H, Ar-H), 10.41 (s,

1H, NH, D₂O exchang.). Anal. Calcd. for C₂₁H₂₃ClN₄O₂S: C, 58.53; H, 5.38; N, 13.00. Found: C, 58.21; H, 5.40; N, 12.60.

4.3.3. 3-[2-[4-(4-Fluorophenyl)piperazin-1-yl]ethyl]-6,7-dihydro-5H-cyclopenta[b]thieno[2,3-d]pyrimidine-2,4-(1H,3H)-dione **6c**

Brown crystal (0.76 g, 37%) m.p. 133–135 °C. ¹H NMR (DMSO-*d*₆); δ 2.35–2.40 (m, 2H, CH₂), 2.70–2.90 (m, 4H, 2CH₂), 3.00–3.70 (m, 10H, 3NCH₂, 2Ar-NCH₂), 3.90–4.10 (t, 2H, CONCH₂), 6.90–7.20 (m, 4H, Ar-H), 10.70 (s, 1H, NH, D₂O exchang.). Anal. Calcd. for C₂₁H₂₃FN₄O₂S: C, 60.85; H, 5.59; N, 13.52. Found: C, 61.25; H, 5.41; N, 13.92.

4.3.4. 3-[2-[4-(2-Methoxyphenyl)piperazin-1-yl]ethyl]-6,7-dihydro-5H-cyclopenta[b]thieno[2,3-d]pyrimidine-2,4-(1H,3H)-dione **6d**

White powder (0.63 g, 30%) m.p. 130–132 °C. ¹H NMR (CDCl₃); δ 2.30–2.40 (m, 2H, CH₂), 2.75–2.90 (m, 4H, 2CH₂), 3.00–3.15 (m, 6H, 3NCH₂), 3.30–3.50 (m, 4H, 2Ar-NCH₂), 3.55–3.65 (t, 2H, CONCH₂), 3.80 (s, 3H, OCH₃), 6.88–7.20 (m, 4H, Ar-H), 10.30 (s, 1H, NH, D₂O exchang.). Anal. Calcd. for C₂₂H₂₆N₄O₃S: C, 61.95; H, 6.14; N, 13.41. Found: C, 62.35; H, 5.80; N, 13.50.

4.3.5. 3-[2-[4-Phenylpiperazin-1-yl]ethyl]-5,6,7,8-tetrahydro-7-methylpyrido[4',3':4,5]thieno[2,3-d]pyrimidine-2,4-(1H,3H)-dione **7a**

White powder (0.74 g, 35%) m.p. 160–161 °C. IR (KBr) ν_{\max} /cm⁻¹ 3220, 3160 (NH), 1648, 1635 (C=O). ¹H NMR (CDCl₃); δ 2.30–3.00 (m, 13H, 2CH₂, NCH₃, 3NCH₂), 3.20–3.55 (m, 6H, CH₂, 2Ar-NCH₂), 3.70–3.80 (t, 2H, CONCH₂), 6.70–7.30 (m, 5H, Ar-H), 10.90 (s, 1H, NH, D₂O exchang.). Anal. Calcd. for C₂₂H₂₇N₅O₂S: C, 62.09; H, 6.40; N, 16.46. Found: C, 61.70; H, 6.05; N, 16.96.

4.3.6. 3-[2-[4-(2-Chlorophenyl)piperazin-1-yl]ethyl]-5,6,7,8-tetrahydro-7-methylpyrido[4',3':4,5]thieno[2,3-d]pyrimidine-2,4-(1H,3H)-dione **7b**

Yellow crystal (0.75 g, 33%) m.p. 118–119 °C. ¹H NMR (DMSO-*d*₆); δ 2.60–3.25 (m, 13H, 2CH₂, NCH₃, 3NCH₂), 3.30–3.65 (m, 6H, CH₂, 2Ar-NCH₂), 3.90–4.00 (t, 2H, CONCH₂), 6.80–7.40 (m, 4H, Ar-H), 11.20 (s, 1H, NH, D₂O exchang.). Anal. Calcd. for C₂₂H₂₆ClN₅O₂S: C, 57.44; H, 5.70; N, 15.22. Found: C, 57.00; H, 5.50; N, 15.65.

4.3.7. 3-[2-[4-(4-Fluorophenyl)piperazin-1-yl]ethyl]-5,6,7,8-tetrahydro-7-methylpyrido[4',3':4,5]thieno[2,3-d]pyrimidine-2,4-(1H,3H)-dione **7c**

Yellowish white crystal (0.88 g, 40%) m.p. 120–122 °C. MS *m/z* (%); 446 (M⁺ + 2, 1.43), 264.5 (14.00), 237 (3.56), 236 (6.66), 192 (100), 179 (5.95), 151 (9.90). Anal. Calcd. for C₂₂H₂₆FN₅O₂S: C, 59.57; H, 5.91; N, 15.79. Found: C, 59.80; H, 6.23; N, 15.30.

4.3.8. 3-[2-[4-(2-Methoxyphenyl)piperazin-1-yl]ethyl]-5,6,7,8-tetrahydro-7-methylpyrido[4',3':4,5]thieno[2,3-d]pyrimidine-2,4-(1H,3H)-dione **7d**

Yellow crystal (0.67 g, 30%) m.p. 130–132 °C. ¹H NMR (DMSO-*d*₆); δ 2.30–2.90 (m, 13H, 2CH₂, NCH₃, 3NCH₂), 3.10–3.40 (m, 6H, CH₂, 2Ar-NCH₂), 3.60–3.70 (t, 2H, CONCH₂), 3.80 (s, 3H, OCH₃), 6.80–7.40 (m, 4H, Ar-H), 10.90–11.00 (br.s, 1H, NH, D₂O exchang.). Anal. Calcd. for C₂₃H₂₉N₅O₃S: C, 60.64; H, 6.42; N, 15.73. Found: C, 60.95; H, 6.10; N, 15.87.

4.4. Ethyl 2-(chloroacetyl-amino)-4,5,6,7-tetrahydro-6-methylthieno[2,3-c]pyridine-3-carboxylate **9 (Scheme 1)**

Chloroacetyl chloride (2.25 g, 20 mmol) was added dropwise under cooling to a solution of ethyl 2-amino-4,5,6,7-tetrahydro-6-methylthieno[2,3-c]pyridine-3-carboxylate **3** (4.80 g, 20 mmol) in chloroform (40 ml). The reaction mixture was heated under reflux for 6 h. The separated solid was filtered while hot dried and

crystallized from ethanol to afford yellow crystal of compound **9** in 3.17 g (50%) yield; m.p. 230–232 °C; ¹H NMR (DMSO-*d*₆); δ 1.20–1.30 (t, 3H, OCH₂CH₃), 2.50–2.80 (m, 7H, 2CH₂, NCH₃), 3.20 (s, 2H, CH₂), 4.20–4.40 (q, 2H, OCH₂CH₃), 4.65 (s, 2H, CH₂Cl), 11.85–11.90 (br s, 1H, NH, D₂O exchang.). MS *m/z* (%); 319 (M⁺ + 2, 2.30), 318 (M⁺ +, 16.20), 317 (M⁺, 7.80), 282 (0.71), 269 (100), 240 (6.60), 224 (0.90). Anal. Calcd. for C₁₃H₁₇ClN₂O₃S: C, 49.29; H, 5.41; N, 8.84. Found: C, 48.98; H, 5.80; N, 9.00.

4.5. Ethyl 2-[[4-substituted phenylpiperazin-1-yl]acetyl-amino]-5,6,7,8-tetrahydro-4H-cyclohepta[b]thiophene-3-carboxylates **10a,b,d,e and ethyl 2-[[4-substituted phenylpiperazin-1-yl]acetyl-amino]-4,5,6,7-tetrahydro-6-methylthieno[2,3-c]pyridine-3-carboxylates **11a,b,d,e** (Scheme 1)**

A mixture of **8** or **9** (3.9 mmol), the appropriate *N*-substituted phenylpiperazine (3.9 mmol) and potassium carbonate (0.539 g, 3.9 mmol) in DMF (10 ml) was heated under reflux for 5 h. The solvent was evaporated under reduced pressure and the residue thus obtained was triturated with water, filtered and dried to give compounds **10** which crystallized from DMF/water and compounds **11** which crystallized from ethanol.

4.5.1. Ethyl 2-[[4-phenylpiperazin-1-yl]acetyl-amino]-5,6,7,8-tetrahydro-4H-cyclohepta[b]thiophene-3-carboxylate **10a**

White needles (1.19 g, 70%) m.p. 160–162 °C. ¹H NMR (CDCl₃); δ 1.33–1.36 (t, 3H, OCH₂CH₃), 1.58–1.66 (m, 4H, 2CH₂), 1.80–1.87 (m, 2H, CH₂), 2.70–2.80 (m, 6H, CH₂, 2NCH₂), 3.00–3.10 (t, 2H, CH₂), 3.29–3.40 (m, 6H, COCH₂, 2Ar-NCH₂), 4.30–4.39 (q, 2H, OCH₂CH₃), 6.80–7.30 (m, 5H, Ar-H), 12.10 (s, 1H, NH, D₂O exchang.). Anal. Calcd. for C₂₄H₃₁N₃O₃S: C, 65.28; H, 7.08; N, 9.52. Found: C, 65.15; H, 6.80; N, 9.99.

4.5.2. Ethyl 2-[[4-(2-chlorophenyl)piperazin-1-yl]acetyl-amino]-5,6,7,8-tetrahydro-4H-cyclohepta[b]thiophene-3-carboxylate **10b**

White needles (1.38 g, 75%) m.p. 115–116 °C. ¹H NMR (CDCl₃); δ 1.33–1.35 (t, 3H, OCH₂CH₃), 1.56–1.62 (m, 4H, 2CH₂), 1.80–1.87 (m, 2H, CH₂), 2.69–2.75 (m, 6H, CH₂, 2NCH₂), 3.00–3.10 (t, 2H, CH₂), 3.27–3.41 (m, 6H, COCH₂, 2Ar-NCH₂), 4.20–4.40 (q, 2H, OCH₂CH₃), 6.88–7.40 (m, 4H, Ar-H), 12.30 (s, 1H, NH, D₂O exchang.). Anal. Calcd. for C₂₄H₃₀ClN₃O₃S: C, 60.55; H, 6.35; N, 8.83. Found: C, 60.91; H, 6.00; N, 9.30.

4.5.3. Ethyl 2-[[4-(2-methoxyphenyl)piperazin-1-yl]acetyl-amino]-5,6,7,8-tetrahydro-4H-cyclohepta[b]thiophene-3-carboxylate **10d**

White crystal (1.38 g, 75%) m.p. 133–135 °C. IR (KBr) ν_{\max} /cm⁻¹ 3240, 3210 (NH), 1750 (COOC₂H₅), 1630 (C=O). MS *m/z* (%); 473 (M⁺ + 1, 3.65), 472 (M⁺, 7.70), 282 (1.80), 233 (2.00), 225 (2.70), 205 (31.30), 150 (100). Anal. Calcd. for C₂₅H₃₃N₃O₄S: C, 63.67; H, 7.05; N, 8.91. Found: C, 63.45; H, 6.60; N, 9.15.

4.5.4. Ethyl 2-[[4-(2-ethoxyphenyl)piperazin-1-yl]acetyl-amino]-5,6,7,8-tetrahydro-4H-cyclohepta[b]thiophene-3-carboxylate **10e**

Yellowish white needles (1.36 g, 73%) m.p. 130–132 °C. ¹H NMR (CDCl₃); δ 1.33–1.38 (m, 6H, 2° CH₂CH₃), 1.55–1.69 (m, 4H, 2CH₂), 1.80–1.87 (m, 2H, CH₂), 2.70–2.79 (m, 6H, CH₂, 2NCH₂), 3.00–3.09 (t, 2H, CH₂), 3.28–3.36 (m, 6H, COCH₂, 2Ar-NCH₂), 4.30–4.38 (m, 4H, 2° CH₂CH₃), 6.89–7.42 (m, 4H, Ar-H), 12.32 (s, 1H, NH, D₂O exchang.). Anal. Calcd. for C₂₆H₃₅N₃O₄S: C, 64.30; H, 7.26; N, 8.62. Found: C, 64.33; H, 7.11; N, 9.00.

4.5.5. Ethyl 2-[[4-phenylpiperazin-1-yl]acetyl-amino]-4,5,6,7-tetrahydro-6-methylthieno[2,3-c]pyridine-3-carboxylate **11a**

White powder (0.68 g, 40%) m.p. 117–118 °C. MS *m/z* (%); 444 (M⁺ + 1, 1.58), 443 (M⁺, 5.05), 442 (M⁺ – 1, 17.52), 282 (3.13), 241

(1.27), 175 (100), 161 (2.20). Anal. Calcd. for $C_{23}H_{30}N_4O_3S$: C, 62.42; H, 6.83; N, 12.66. Found: C, 62.10; H, 6.65; N, 13.00.

4.5.6. Ethyl 2-[[4-(2-chlorophenyl)piperazin-1-yl]acetyl]amino]-4,5,6,7-tetrahydro-6-methylthieno[2,3-c]pyridine-3-carboxylate **11b**

Yellowish white crystal (0.72 g, 39%) m.p. 120–121 °C. 1H NMR ($CDCl_3$); δ 1.20–1.30 (t, 3H, OCH_2CH_3), 2.40–2.90 (m, 11H, 2CH₂, NCH₃, 2NCH₂), 3.00–3.65 (m, 8H, CH₂, COCH₂, 2Ar-NCH₂), 4.20–4.40 (q, 2H, OCH_2CH_3), 6.90–7.40 (m, 4H, Ar-H), 12.20–12.40 (br s, 1H, NH, D_2O exchang.). Anal. Calcd. for $C_{23}H_{29}ClN_4O_3S$: C, 57.91; H, 6.13; N, 11.75. Found: C, 58.22; H, 6.44; N, 12.00.

4.5.7. Ethyl 2-[[4-(2-methoxyphenyl)piperazin-1-yl]acetyl]amino]-4,5,6,7-tetrahydro-6-methylthieno[2,3-c]pyridine-3-carboxylate **11d**

White crystal (0.65 g, 36%) m.p. 125–127 °C. IR (KBr) ν_{max}/cm^{-1} 3210 (NH), 1745 ($COOC_2H_5$), 1640 (C=O). MS m/z (%); 473 (M^+ , 0.53), 472 ($M^+ - 1$, 1.89), 367 (1.07), 282 (0.40), 240 (1.52), 233 (0.71), 150 (100). Anal. Calcd. for $C_{24}H_{32}N_4O_4S$: C, 60.99; H, 6.82; N, 11.86. Found: C, 60.65; H, 6.59; N, 12.10.

4.5.8. Ethyl 2-[[4-(2-ethoxyphenyl)piperazin-1-yl]acetyl]amino]-4,5,6,7-tetrahydro-6-methylthieno[2,3-c]pyridine-3-carboxylate **11e**

White crystal (0.75 g, 40%) m.p. 110–111 °C. 1H NMR ($CDCl_3$); δ 1.30–1.42 (m, 6H, 2° CH_2CH_3), 2.20–3.00 (m, 11H, 2CH₂, NCH₃, 2NCH₂), 3.20–3.70 (m, 8H, CH₂, COCH₂, 2Ar-NCH₂), 4.30–4.48 (m, 4H, 2° CH_2CH_3), 6.99–7.55 (m, 4H, Ar-H), 12.21–12.30 (br s, 1H, NH, D_2O exchang.). Anal. Calcd. for $C_{25}H_{34}N_4O_4S$: C, 61.70; H, 7.04; N, 11.51. Found: C, 61.49; H, 7.11; N, 11.90.

4.6. 3-Amino-2-[[4-substituted phenyl]piperazin-1-yl]methyl]-6,7,8,9-tetrahydro-5H-cyclohepta[b]thieno[2,3-d]pyrimidin-4(3H)-ones **12a,b,d,e (Scheme 1)**

A mixture of ethyl 2-[[4-(substituted phenyl)piperazin-1-yl]acetyl]amino]-5,6,7,8-tetrahydro-4H-cyclohepta[b]thiophene-3-carboxylate **10** (2.1 mmol) and 99% hydrazine hydrate (4.0 g, 80 mmol) in absolute ethanol (10 ml) was heated under reflux for 12 h. The separated solid was filtered while hot, dried and crystallized from DMF/water to afford compounds **12**.

4.6.1. 3-Amino-2-[[4-phenyl]piperazin-1-yl]methyl]-6,7,8,9-tetrahydro-5H-cyclohepta[b]thieno[2,3-d]pyrimidin-4(3H)-one **12a**

Yellowish white needles (0.38 g, 50%) m.p. 170–172 °C. IR (KBr) ν_{max}/cm^{-1} 3280 (NH₂), 1632 (C=O). 1H NMR ($CDCl_3$); δ 1.60–1.75 (m, 4H, 2CH₂), 1.83–1.94 (m, 2H, CH₂), 2.70–2.90 (m, 6H, CH₂, 2NCH₂), 3.10–3.36 (m, 6H, CH₂, 2Ar-NCH₂), 3.80 (s, 2H, CH₂ attached to piperazine moiety), 6.30–6.39 (br s, 2H, NH₂, D_2O exchang.), 6.90–7.30 (m, 5H, Ar-H). Anal. Calcd. for $C_{22}H_{27}N_5OS$: C, 64.52; H, 6.64; N, 17.10. Found: C, 64.92; H, 6.50; N, 17.60.

4.6.2. 3-Amino-2-[[4-(2-chlorophenyl)piperazin-1-yl]methyl]-6,7,8,9-tetrahydro-5H-cyclohepta[b]thieno[2,3-d]pyrimidin-4(3H)-one **12b**

White powder (0.41 g, 45%) m.p. 140–143 °C. 1H NMR ($CDCl_3$); δ 1.65–1.75 (m, 4H, 2CH₂), 1.87–1.93 (m, 2H, CH₂), 2.75–2.87 (m, 6H, CH₂, 2NCH₂), 3.00–3.12 (t, 2H, CH₂), 3.24–3.35 (m, 4H, 2Ar-NCH₂), 3.81 (s, 2H, CH₂ attached to piperazine moiety), 6.42–6.48 (br s, 2H, NH₂, D_2O exchang.), 6.84–7.00 (m, 4H, Ar-H). Anal. Calcd. for $C_{22}H_{26}ClN_5OS$: C, 59.51; H, 5.90; N, 15.77. Found: C, 59.80; H, 6.25; N, 16.15.

4.6.3. 3-Amino-2-[[4-(2-methoxyphenyl)piperazin-1-yl]methyl]-6,7,8,9-tetrahydro-5H-cyclohepta[b]thieno[2,3-d]pyrimidin-4(3H)-one **12d**

White powder (0.38 g, 42%) m.p. 160–162 °C. MS m/z (%); 439.45 (M^+ , 6.53), 411 (100), 250 (2.45), 237 (18.57), 221 (8.16), 209 (1.63),

193 (31.02). Anal. Calcd. For $C_{23}H_{29}N_5O_2S$: C, 62.84; H, 6.65; N, 15.93. Found: C, 62.65; H, 6.40; N, 16.30.

4.6.4. 3-Amino-2-[[4-(2-ethoxyphenyl)piperazin-1-yl]methyl]-6,7,8,9-tetrahydro-5H-cyclohepta[b]thieno[2,3-d]pyrimidin-4(3H)-one **12e**

Brown powder (0.49 g, 45%) m.p. 150–152 °C. 1H NMR ($CDCl_3$); δ 1.42–1.48 (t, 3H, OCH_2CH_3), 1.66–1.74 (m, 4H, 2CH₂), 1.86–1.93 (m, 2H, CH₂), 2.71–2.88 (m, 6H, CH₂, 2NCH₂), 3.00–3.20 (t, 2H, CH₂), 3.26–3.34 (m, 4H, 2Ar-NCH₂), 3.81 (s, 2H, CH₂ attached to piperazine moiety), 4.00–4.10 (q, 2H, OCH_2CH_3), 6.40–6.49 (br s, 2H, NH₂, D_2O exchang.), 6.83–7.0 (m, 4H, Ar-H). Anal. Calcd. For $C_{24}H_{31}N_5O_2S$: C, 63.55; H, 6.89; N, 15.44. Found: C, 63.10; H, 7.00; N, 15.86.

4.7. 1-Chloromethyl-4-phenyl-6,7,8,9-tetrahydro-[1,2,4]triazolo[4,3-a]benzo[b]thieno[3,2-e]pyrimidin-5(4H)-one **16 (Scheme 2)**

Chloroacetyl chloride (5.64 g, 0.05 mol) was added dropwise under cooling to a solution of **15** (7.80 g, 0.025 mol) in chloroform (30 ml). The reaction mixture was heated under reflux for 4 h. The separated solid was filtered, dried and crystallized from ethanol to give red crystal of compound **16** in 4.16 g (45%); m.p. 253–255 °C. IR (KBr) ν_{max}/cm^{-1} 1640 (C=O), 1552, 1503 (C=N). 1H NMR ($DMSO-d_6$); δ 1.75–1.82 (m, 4H, 2CH₂), 2.80–2.90 (m, 4H, 2CH₂), 4.65 (s, 2H, CH₂Cl), 7.50–7.70 (m, 5H, Ar-H). MS m/z (%); 372 ($M^+ + 1$, 6.87), 371 (M^+ , 5.63), 322 (2.53), 295 (1.12), 283 (7.06), 206 (0.15), 57 (100). Anal. Calcd. for $C_{18}H_{15}ClN_4OS$ (370.86): C, 58.30; H, 4.08; N, 15.11. Found: C, 58.00; H, 4.54; N, 15.60.

4.8. 1-[[4-Substituted phenyl]piperazin-1-yl]methyl]-4-phenyl-6,7,8,9-tetrahydro-[1,2,4]triazolo[4,3-a]benzo[b]thieno[3,2-e]pyrimidin-5(4H)-ones **17a–e (Scheme 2)**

A mixture of 1-chloromethyl-4-phenyl-6,7,8,9-tetrahydro-[1,2,4]triazolo[4,3-a]benzo[b]thieno[3,2-e]pyrimidin-5(4H)-one **16** (1.44 g, 3.9 mmol), the appropriate *N*-substituted phenylpiperazine (3.9 mmol) and potassium carbonate (0.539 g, 3.9 mmol) in DMF (10 ml) was heated under reflux for 6 h. The solvent was evaporated under reduced pressure. The residue thus formed was triturated with water, filtered, dried and crystallized from aqueous ethanol to afford compounds **17a,c,d** or crystallized from DMF to afford compounds **17b,e**.

4.8.1. 1-[[4-Phenyl]piperazin-1-yl]methyl]-4-phenyl-6,7,8,9-tetrahydro-[1,2,4]triazolo[4,3-a]benzo[b]thieno[3,2-e]pyrimidin-5(4H)-one **17a**

Brown powder (0.77 g, 40%) m.p. 133–135 °C. MS m/z (%); 499 ($M^+ + 2$, 0.59), 498 ($M^+ + 1$, 1.41), 421 (0.44), 336 (10.69), 161 (14.03), 145 (100), 77 (20.49). Anal. Calcd. for $C_{28}H_{28}N_6OS$: C, 67.72; H, 5.68; N, 16.92. Found: C, 67.23; H, 5.98; N, 17.30.

4.8.2. 1-[[4-(2-Chlorophenyl)piperazin-1-yl]methyl]-4-phenyl-6,7,8,9-tetrahydro-[1,2,4]triazolo[4,3-a]benzo[b]thieno[3,2-e]pyrimidin-5(4H)-one **17b**

Yellow crystal (1.13 g, 55%) m.p. 311–312 °C. 1H NMR ($CDCl_3$); δ 1.75–1.90 (m, 4H, 2CH₂), 2.70–3.00 (m, 8H, 2CH₂ and 2NCH₂), 3.20–3.40 (m, 4H, 2Ar-NCH₂), 4.15 (s, 2H, CH₂ attached to piperazine moiety), 6.90–7.90 (m, 9H, Ar-H). Anal. Calcd. for $C_{28}H_{27}ClN_6OS$: C, 63.30; H, 5.12; N, 15.82. Found: C, 63.00; H, 5.50; N, 16.20.

4.8.3. 1-[[4-(4-Fluorophenyl)piperazin-1-yl]methyl]-4-phenyl-6,7,8,9-tetrahydro-[1,2,4]triazolo[4,3-a]benzo[b]thieno[3,2-e]pyrimidin-5(4H)-one **17c**

Yellow powder (0.78 g, 39%) m.p. 290–292 °C. ¹H NMR (CDCl₃); δ 1.75–1.90 (m, 4H, 2CH₂), 2.65–2.90 (m, 8H, 2CH₂ and 2NCH₂), 3.20–3.30 (m, 4H, 2Ar-NCH₂), 3.75 (s, 2H, CH₂ attached to piperazine moiety), 7.00–7.80 (m, 9H, Ar-H). Anal. Calcd. for C₂₈H₂₇FN₆O: C, 65.35; H, 5.29; N, 16.33. Found: C, 65.20; H, 5.59; N, 16.70.

4.8.4. 1-[[4-(2-Methoxyphenyl)piperazin-1-yl]methyl]-4-phenyl-6,7,8,9-tetrahydro-[1,2,4]triazolo[4,3-a]benzo[b]thieno[3,2-e]pyrimidin-5(4H)-one **17d**

Brown crystal (0.86 g, 42%) m.p. 301–303 °C. ¹H NMR (DMSO-d₆); δ 1.50–1.80 (m, 4H, 2CH₂), 2.70–2.80 (m, 8H, 2CH₂ and 2NCH₂), 2.95–3.10 (m, 4H, 2Ar-NCH₂), 3.80 (s, 2H, CH₂ attached to piperazine moiety), 3.90 (s, 3H, OCH₃), 6.70–7.60 (m, 9H, Ar-H). Anal. Calcd. for C₂₉H₃₀N₆O₂S: C, 66.14; H, 5.74; N, 15.96. Found: C, 66.44; H, 5.54; N, 16.40.

4.8.5. 1-[[4-(2-Ethoxyphenyl)piperazin-1-yl]methyl]-4-phenyl-6,7,8,9-tetrahydro-[1,2,4]triazolo[4,3-a]benzo[b]thieno[3,2-e]pyrimidin-5(4H)-one **17e**

White powder (1.05 g, 50%) m.p. 150–152 °C. ¹H NMR (CDCl₃); δ 1.35–1.50 (t, 3H, OCH₂CH₃), 1.70–1.88 (m, 4H, 2CH₂), 2.70–2.96 (m, 8H, 2CH₂ and 2NCH₂), 3.08–3.21 (m, 4H, 2Ar-NCH₂), 3.72 (s, 2H, CH₂ attached to piperazine moiety), 4.00–4.15 (q, 2H, OCH₂CH₃), 6.87–7.40 (m, 9H, Ar-H). Anal. Calcd. for C₃₀H₃₂N₆O₂S: C, 66.64; H, 5.97; N, 15.54. Found: C, 67.00; H, 5.51; N, 15.90.

4.9. Ethyl 2-(benzoylthioureido)-5,6,7,8-tetrahydro-4H-cyclohepta[b]thiophene-3-carboxylate **18** (Scheme 2)

Benzoyl chloride (3.37 g, 24 mmol) was added to a solution of ammonium thiocyanate (2.58 g, 34 mmol) in anhydrous acetone (15 ml) and the resulting suspension was heated under reflux for 10 min. A solution of ethyl 2-amino-5,6,7,8-tetrahydro-4H-cyclohepta[b]thiophene-3-carboxylate **2** (5.74 g, 24 mmol) in anhydrous acetone (60 ml) was added to the previous suspension and the reaction mixture was heated under reflux for another 10 min. After cooling, the separated solid was collected by filtration, poured into water and filtered. The solid obtained was dried and crystallized from acetone to afford compound **18** in 6.76 g (70%); m.p. 152–3 °C. ¹H NMR (CDCl₃); δ 1.40–1.48 (t, 3H, OCH₂CH₃), 1.60–1.70 (m, 4H, 2CH₂), 1.82–1.89 (m, 2H, CH₂), 2.77–2.80 (t, 2H, CH₂), 3.00–3.10 (t, 2H, CH₂), 4.45–4.58 (q, 2H, OCH₂CH₃), 7.50–7.90 (m, 5H, Ar-H), 9.00–9.10 (br s, 1H, NH, D₂O exchange), 14.50–14.60 (br s, 1H, NH, D₂O exchange). MS *m/z* (%): 405 (M⁺ + 2, 0.99), 404 (M⁺ + 1, 2.04), 403 (M⁺, 2.95), 325 (0.99), 297 (1.36), 239 (27.77), 105 (100). Anal. Calcd. for C₂₀H₂₂N₂O₃S₂: C, 59.68; H, 5.51; N, 6.96. Found: C, 59.23; H, 5.32; N, 7.40.

4.10. Potassium salt of 2-mercapto-6,7,8,9-tetrahydro-5H-cyclohepta[b]thieno[2,3-d]pyrimidin-4(3H)-one **19** (Scheme 2)

A mixture of the thioureido derivative **18** (3.46 g, 8.6 mmol) and potassium hydroxide (0.48 g, 8.6 mmol) in absolute ethanol (35 ml) was heated under reflux for 3 h. The separated solid was filtered while hot, dried and crystallized from *n*-butanol to give compound **19** in 1.74 g (70%); m.p. 315–317 °C. ¹H NMR (DMSO-d₆); δ 1.46–1.60 (m, 4H, 2CH₂), 1.70–1.80 (m, 2H, CH₂), 2.59–2.61 (t, 2H, CH₂), 3.08–3.10 (t, 2H, CH₂), 10.15–10.22 (br s, 1H, NH, D₂O exchange). Anal. Calcd. for C₁₁H₁₁KN₂O₂S₂: C, 45.49; H, 3.82; N, 9.64. Found: C, 45.79; H, 3.50; N, 10.15.

4.11. 2-[[4-Substituted phenyl]piperazin-1-yl]carbonylmethylthio]-6,7,8,9-tetrahydro-5H-cyclohepta[b]thieno[2,3-d]pyrimidin-4(3H)-ones **21a,b,d,e** (Scheme 2)

1-Chloroacetyl-4-(substituted phenyl)piperazine derivative **20** (3.6 mmol) was added to a suspension of compound **19** (0.87 g, 3 mmol) in DMF (15 ml) and the reaction mixture was heated under reflux for 10 h. After cooling, the separated solid was collected by filtration, dried and crystallized from DMF.

4.11.1. 2-[[4-Phenylpiperazin-1-yl]carbonylmethylthio]-6,7,8,9-tetrahydro-5H-cyclohepta[b]thieno[2,3-d]pyrimidin-4(3H)-ones **21a**

Yellow powder (0.65 g, 40%) m.p. 245–246 °C. ¹H NMR (DMSO-d₆); δ 1.47–1.60 (m, 4H, 2CH₂), 1.75–1.82 (m, 2H, CH₂), 2.67–2.75 (t, 2H, CH₂), 3.05–3.25 (m, 6H, CH₂, 2NCH₂), 3.56–3.71 (m, 4H, 2Ar-NCH₂), 4.23 (s, 2H, CH₂CO), 6.74–7.30 (m, 5H, Ar-H), 12.59–12.63 (br s, 1H, NH, D₂O exchange). Anal. Calcd. for C₂₃H₂₆N₄O₂S₂: C, 60.77; H, 5.76; N, 12.32. Found: C, 61.10; H, 5.99; N, 12.00.

4.11.2. 2-[[4-(2-Chlorophenyl)piperazin-1-yl]carbonylmethylthio]-6,7,8,9-tetrahydro-5H-cyclohepta[b]thieno[2,3-d]pyrimidin-4(3H)-ones **21b**

White powder (0.61 g, 35%) m.p. 245–246 °C. ¹H NMR (CDCl₃); δ 1.52–1.73 (m, 4H, 2CH₂), 1.82–1.92 (m, 2H, CH₂), 2.75–2.82 (t, 2H, CH₂), 3.02–3.30 (m, 6H, CH₂, 2NCH₂), 3.65–3.83 (m, 4H, 2Ar-NCH₂), 4.15 (s, 2H, CH₂CO), 6.76–7.33 (m, 4H, Ar-H), 12.60–12.68 (br s, 1H, NH, D₂O exchange). Anal. Calcd. for C₂₃H₂₅ClN₄O₂S₂: C, 56.49; H, 5.15; N, 11.46. Found: C, 56.80; H, 4.80; N, 11.95.

4.11.3. 2-[[4-(2-Methoxyphenyl)piperazin-1-yl]carbonylmethylthio]-6,7,8,9-tetrahydro-5H-cyclohepta[b]thieno[2,3-d]pyrimidin-4(3H)-ones **21d**

Brown crystal (0.78 g, 45%) m.p. 230–232 °C. IR (KBr) ν_{\max} /cm⁻¹ 3310 (NH), 1670, 1643 (C=O), 1150 (C–S–C). MS *m/z* (%): 485 (M⁺, 1.87), 378 (1.75), 294 (5.02), 234 (7.58), 220 (1.98), 191 (5.25), 133 (100). Anal. Calcd. for C₂₄H₂₈N₄O₃S₂: C, 59.48; H, 5.82; N, 11.56. Found: C, 59.70; H, 6.10; N, 11.71.

4.11.4. 2-[[4-(2-Ethoxyphenyl)piperazin-1-yl]carbonylmethylthio]-6,7,8,9-tetrahydro-5H-cyclohepta[b]thieno[2,3-d]pyrimidin-4(3H)-ones **21e**

Brown powder (0.71 g, 40%) m.p. 220–221 °C. ¹H NMR (CDCl₃); δ 1.28–1.34 (t, 3H, OCH₂CH₃), 1.54–1.76 (m, 4H, 2CH₂), 1.84–1.93 (m, 2H, CH₂), 2.74–2.80 (t, 2H, CH₂), 2.90–3.30 (m, 6H, CH₂, 2NCH₂), 3.69–3.88 (m, 4H, 2Ar-NCH₂), 4.20 (s, 2H, CH₂CO), 4.25–4.30 (q, 2H, OCH₂CH₃), 6.70–7.32 (m, 4H, Ar-H), 12.40–12.45 (br s, 1H, NH, D₂O exchange). Anal. Calcd. for C₂₅H₃₀N₄O₃S₂: C, 60.21; H, 6.06; N, 11.24. Found: C, 60.55; H, 6.40; N, 11.65.

5. Pharmacology

5.1. 5-HT_{2A} antagonist activity

5.1.1. Materials and animals

Some of the prepared compounds were screened for 5-HT_{2A} antagonist activity using isolated pulmonary arterial rings of rats [28–30]. Adult Sprague-Dawley rats of both sexes weighing 200–250 g were used in this experiment. They were purchased from local source. Animals were maintained under standard conditions of temperature with regular 12 h light/12 h dark cycle and allowed free access to standard laboratory food and water. Diethylether was used to anesthetize the animals. A physiological salt solution (PSS) in mM/l composed of: NaCl, 118; KCl, 4.7; CaCl₂·2H₂O, 2.5; KH₂PO₄, 1.2; MgSO₄·7H₂O, 1.2; NaHCO₃, 25; and glucose, 10 was used to

maintain the arterial rings of rats in it [28–30]. Serotonin creatinine sulfate monohydrate (5-HT), as white powder (Fluka Chemie, Steinheim, Switzerland) was used an agonist. risperidone was used as the standard drug. 5-HT, risperidone and the tested compounds were freshly prepared by dissolving in water just before use in 10^{-4} molar concentration.

5.1.2. Methods

Rats were killed by an overdose of diethylether. The chest was opened along the right side of the sternum after cutting the diaphragm. The pulmonary artery was tied gently, then separated and rapidly placed in warm physiological salt solution (PSS). The pulmonary artery was trimmed and cut into rings. The rings were cleaned of connective tissue with care taken not to touch the luminal surface. Each ring was suspended horizontally between two stainless steel parallel hooks, one of which was fixed and the other attached to isometric tension transducer for the measurement of isometric tension in an organ bath filled with 50 ml of PSS at fixed temperature of 37°C and continuously bubbled with 100% pure O_2 . The suspended pulmonary arterial ring was allowed to equilibrate for 30 min under a resting load of 3 g. Isometric tension generated by the vascular smooth muscles was measured using a displacement transducer (model 50-7905, Harvard apparatus LTD, South Natick, MA, USA) and recorded on a two-channel oscillograph (model 50-8622, Harvard Apparatus Ltd, USA).

A dose of 5-HT, 10^{-4} M, was applied and allowed to act till the pressor response was fully developed. The pulmonary arterial ring was washed with PSS. A concentration of 10^{-4} M of the test compounds or risperidone was applied and incubated for 5 min in the organ bath to evaluate its activity on the 5-HT_{2A} receptors. 5-HT was added in the organ bath in the presence of the test compounds in order to evaluate the antagonistic activity on the 5-HT_{2A} receptors. The activities of the tested compounds are shown in Table 1.

6. Molecular modeling methods

6.1. Conformational search

Initial structures for the molecules **6a**, **11d**, **21a** and **17a** were constructed using the HyperChem program version 5.1 [56]. The MM+ [59,60] (calculations in vacuo, bond dipole option for electrostatics, Polak–Ribiere algorithm, and RMS gradient of 0.01 kcal/mol) conformational searching in torsional space was performed using the multiconformer method [63]. Energy minima for compounds **6a**, **11d**, **21a** and **17a** were determined by a semi-empirical method AM1 [61] (as implemented in HyperChem 5.1). The conformations thus obtained were confirmed as minima by vibrational analysis. Atom-centered charges for each molecule were computed from the AM1 wave functions (HyperChem 5.1) by the procedure of Orozco and Luque [64], which provides derived charges that closely resemble those obtainable from ab initio 6-31G⁺ calculations.

6.2. Flexible alignment and pharmacophore prediction

Flexible alignment and pharmacophore prediction of compounds **6a**, **11d**, **21a** and **17a** was carried out with the software 'Molecular Operating Environment' (MOE of Chemical Computing Group Inc., on a Core 2 duo 1.83 GHz workstation) [68]. The molecules were built using the Builder module of MOE. Their geometry was optimized by using the MMFF94 force-field followed by a flexible alignment using systematic conformational search. Lowest energy aligned conformation(s) were identified through the analysis module of DSV by Accelrys Inc. [71], and the distances and angles between the pharmacophoric elements were measured.

Acknowledgments

Our sincere acknowledgments to Chemical Computing Group Inc, 1010 Sherbrooke Street West, Suite 910, Montreal H3A 2R7, Canada, for using the package of MOE 2008.10 software. Also, our deep thanks are due to all members of Pharmacology Department, Faculty of Pharmacy, Mansoura University, for their aid in the *in vitro* biological evaluations.

References

- [1] F. Saudou, R. Hen, Med. Chem. Res. 4 (1994) 16.
- [2] J. Bockaert, L. Fagni, A. Dumuis, in: H.G. Baumgarten, M. Göthert (Eds.), Serotonergic Neurons and 5-HT Receptors in the CNS, Springer, Berlin, 1997, p. 439.
- [3] L.M. Gaster, F.D. King, Med. Res. Rev. 17 (1997) 163.
- [4] A. Dumuis, H. Ansanay, C. Waeber, M. Sebben, L. Fagni, J. Bockaert, in: O. Olivier, I. van Wijngaarden, W. Soudijn (Eds.), Serotonin Receptors and Their Ligands, Elsevier, Amsterdam, 1997, p. 261.
- [5] M.L. López-Rodríguez, M. Murcia, B. Benhamú, A. Viso, M. Campillo, L. Pardo, Bioorg. Med. Chem. Lett. 11 (2001) 2807.
- [6] H.G. Baumgarten, M. Göthert, Serotonergic Neurons and 5-HT Receptors in the CNS, In: Handbook of Experimental Pharmacology, vol. 129. Springer, Berlin, 1997.
- [7] G.R. Martin, R.M. Eglen, D. Hoyer, M.W. Hamblin, F. Yocca, Advances in serotonin receptor research: molecular biology, signal transmission, and therapeutics. Ann. N.Y. Acad. Sci. (1998) New York.
- [8] N.M. Barnes, T. Sharp, Neuropharmacology 38 (1999) 1083.
- [9] D. Hoyer, J.P. Hannon, G.R. Martin, Pharmacol. Biochem. Behav. 71 (2002) 533.
- [10] M. Berger, J.A. Gray, B.L. Roth, Annu. Rev. Med. 60 (2009) 355.
- [11] K. Lesch, D. Bengel, A. Heils, S.Z. Sabol, B.D. Greenberg, S. Petri, R. Clemens, J.B. Müller, D.H. Hamer, D.L. Murphy, Science 274 (1996) 1527.
- [12] A. Caspi, K. Sugden, T.E. Moffitt, A. Taylor, I.W. Craig, W. Harrington, J. McClay, J. Mill, J. Martin, A. Braithwaite, R. Poulton, Science 301 (2003) 386.
- [13] N. Caspi, I. Modai, P. Barak, A. Waisbourd, H. Zbarsky, S. Hirschmann, M. Ritsner, Int. Clin. Psychopharmacol. 16 (2001) 111.
- [14] G. Basky, Can. Med. Assoc. J. 162 (2000) 1343.
- [15] B.M. Ramadnan, P. Carine, H. Judith, J.M.T. Mathilda, K. Ronald, J.A.K. Suzanne, W.N.A. Jan, C. Edwin, D.B. Alain, Am. J. Physiol. Gastrointest. Liver Physiol. 296 (2009) G963.
- [16] D. Hoyer, D.E. Hannon, J.R. Fozard, Pharmacol. Rev. 46 (1994) 157.
- [17] A.J. Robichaud, B.L. Largent, Annu. Rep. Med. Chem. 35 (2000) 11.
- [18] D.A. Evrard, B.L. Harrison, Annu. Rep. Med. Chem. 34 (1999) 1.
- [19] D. Hoyer, G. Martin, Neuropharmacology 36 (1997) 419.
- [20] A. Carlsson, N. Waters, M.L. Carlsson, Biol. Psychiatry 46 (1999) 1388.
- [21] S.F. Leibowitz, J.T. Alexander, Biol. Psychiatry 44 (1998) 851.
- [22] R.E. Gregory, D.S. Ettinger, Drugs 55 (1998) 173.
- [23] J.G. Jin, A.E. Fox-Orenstein, J.R. Grider, J. Pharmacol. Exp. Ther. 288 (1999) 93.
- [24] L.L. Bruntton, J.S. Lazo, K.L. Parker, 5-Hydroxytryptamine (serotonin): receptor agonists and antagonists, Goodman and Gilman's The Pharmacological Basis of Therapeutics, 11th ed. McGraw-Hill, New York, 2006, p. 297.
- [25] L. Rodat-Despoix, H. Crevel, R. Marthan, J.-P. Savineau, C.J. Guiber, Vasc. Res. 45 (2008) 181.
- [26] M.R. MacLean, G. Sweeney, M. Baird, K.M. McCulloch, M. Houslay, I. Morecroft, Br. J. Pharmacol. 119 (1996) 917.
- [27] E. Nozik-Grayck, T.J. McMahon, Y.-C.T. Huang, C.S. Dieterle, J.S. Stamler, C.A. Piantadosi, Am. J. Physiol. Lung Cell. Mol. Physiol. 282 (2002) L1057.
- [28] D. Al-Agmy, N. El-Laban, H. El-Kashef, J. Basic Appl. Sci. 2 (2006) 11.
- [29] M.N. Nagi, P. Leaf, G.R. Marlin, M. Morse, Br. J. Pharmacol. 89 (1986) 493.
- [30] M. El-Mazar, N.M. Gameil, H.A. El-Kashef, N.A. El-Laban, Banha Med. J. (1995) 12.
- [31] J.H. Block, J.M. Beal Jr., Central nervous system depressants, Wilson and Gisvold's Textbook of Organic Medicinal and Pharmaceutical Chemistry, 11th ed. Lippincott Williams and Wilkins, Philadelphia, 2004, p. 501.
- [32] A. Kerwin, S. Osborne, Psychiatry 4 (2005) 36.
- [33] C.G. Wermuth, Pharmacophore identification and receptor mapping, The Practice of Medicinal Chemistry, second ed. Academic Press, London, 2003, p. 387.
- [34] M.F. Hibert, M.W. Gittos, D.N. Middlemiss, A.K. Mir, J.R. Fozard, J. Med. Chem. 31 (1988) 1087.
- [35] M.L. Lopez-Rodríguez, M.J. Morcillo, T.K. Rovat, E. Fernandez, A.M. Sanz, L. Orensanz, Bioorg. Med. Chem. Lett. 8 (1998) 581.
- [36] G. Romeo, G. Ambrosini, S. Guccione, A. De Blasi, F. Russo, Eur. J. Med. Chem. 28 (1993) 499.
- [37] M. Modica, M. Santagati, F. Russo, L. Parotti, L. De Gioia, C. Selvaggini, M. Salmona, T. Mennini, J. Med. Chem. 40 (1997) 574.
- [38] Y. Liao, H. Böttcher, J. Harting, H. Greiner, C. Amsterdam, T. Cremers, S. Sundell, J. März, W. Rautenberg, H. Wikström, J. Med. Chem. 43 (2000) 517.
- [39] R.B. Westkaemper, R.A. Glennon, Curr. Top. Med. Chem. 2 (2002) 575.
- [40] L. Santana, E. Uriarte, Y. Fall, M. Teixeira, C. Terán, E. García-Martínez, B.-R. Tolf, Eur. J. Med. Chem. 37 (2002) 503.
- [41] S.M. Bromidge, S. Dabbs, D.T. Davies, S. Davies, D.M. Duckworth, I.T. Forbes, A. Gadre, P. Ham, G.E. Jones, F.D. King, D.V. Saunders, K.M. Thewlis, D. Vyas,

- T.P. Blackburn, V. Holland, G.A. Kennett, G.J. Riley, M.D. Wood, *Bioorg. Med. Chem.* 7 (1999) 2767.
- [42] F.M. Awadallah, *Sci. Pharm.* 76 (2008) 415.
- [43] A. Bronowska, A. Leś, Z. Chilmoneczyk, S. Filipek, Ø. Edvardsen, R. Østensen, I. Sylte, *Bioorg. Med. Chem.* 9 (2001) 881.
- [44] Z. Chilmoneczyk, M. Cybulski, J. Iskra-Jopa, E. Chojnacka-Wójcik, E. Tatarczyńska, A. Kłodzińska, A. Leś, A. Bronowska, I. Sylte, *Il Farmaco* 57 (2002) 285.
- [45] Z. Chilmoneczyk, *Il Farmaco* 55 (2000) 191.
- [46] D. Hamprecht, F. Micheli, G. Tedesco, A. Checchia, D. Donati, M. Petrone, S. Terreni, M. Wood, *Bioorg. Med. Chem. Lett.* 17 (2007) 428.
- [47] F. Micheli, A. Pasquarello, G. Tedesco, D. Hamprecht, G. Bonanomi, A. Checchia, A. Jaxa-Chamiec, F. Damiani, S. Davalli, D. Donati, C. Gallotti, M. Petrone, M. Rinaldi, G. Riley, S. Terreni, M. Wood, *Bioorg. Med. Chem. Lett.* 16 (2006) 3906.
- [48] R.V. Perumal, R. Mahesh, *Bioorg. Med. Chem. Lett.* 16 (2006) 2769.
- [49] M.L. López-Rodríguez, B. Benhamú, A. Viso, M.J. Morcillo, M. Murcia, L. Orensanz, M.J. Alfaro, M.I. Martín, *Bioorg. Med. Chem.* 7 (1999) 2271.
- [50] K.G. Liu, J.R. Lo, T.A. Comery, G.M. Zhang, J.Y. Zhang, D.M. Kowal, D.L. Smith, L. Di, E.H. Kerns, L.E. Schechter, A.J. Robichaud, *Bioorg. Med. Chem. Lett.* 19 (2009) 2413.
- [51] M.L. López-Rodríguez, E. Porras, B. Benhamú, J.A. Ramos, M.J. Morcillo, J.L. Lavandera, *Bioorg. Med. Chem. Lett.* 10 (2000) 1097.
- [52] K. Gewald, E. Schinke, H. Bottcher, *Chem. Ber.* 99 (1966) 94.
- [53] E. Kretzschmar, G. Laban, P. Meisel, R. Grupe, W. Kirsten, Ger. (East) Patent DD 272,082, 1989; *Chem. Abstr.* 112 (1990) 198357u.
- [54] M. Perrissin, C.L. Duc, G. Narcisse, F. Bakri-Logeais, F. Huguët, *Eur. J. Med. Chem.* 15 (1980) 413.
- [55] M.L. López-Rodríguez, D. Ayala, A. Viso, B. Benhamú, R. Fernández de la Pradilla, F. Zarza, J.A. Ramos, *Bioorg. Med. Chem.* 12 (2004) 1551.
- [56] HyperChem Version 5.1. Hypercube Inc., 1995–2009.
- [57] M.L. López-Rodríguez, B. Benhamú, M.J. Morcillo, I. Tejada, D. Avila, I. Marco, L. Schiapparelli, D. Frechilla, J. Del Río, *Bioorg. Med. Chem. Lett.* 13 (2003) 3177.
- [58] M.A.H. Ismail, M.N.Y. Aboul-Enein, K.A.M. Abouzid, R.A.T. Serya, *Bioorg. Med. Chem.* 14 (2006) 898.
- [59] S. Profeta, N.L. Allinger, *J. Am. Chem. Soc.* 107 (1985) 1907.
- [60] N.L. Allinger, *J. Am. Chem. Soc.* 99 (1977) 8127.
- [61] M.J.S. Dewar, E.G. Zoebisch, E.F. Healy, J.J.P. Stewart, *J. Am. Chem. Soc.* 107 (1985) 3902.
- [62] A.A.-M. Abdel-Aziz, *Eur. J. Med. Chem.* 42 (2007) 614.
- [63] M. Lipton, W.C. Still, *J. Comput. Chem.* 9 (1988) 345.
- [64] M. Orozco, F.J. Luque, *J. Comput. Chem.* 11 (1990) 909.
- [65] A.A.-M. Abdel-Aziz, *Tetrahedron Lett.* 48 (2007) 2861.
- [66] P. Labute, C. Williams, M. Feher, E. Sourial, J.M. Schmidt, *J. Med. Chem.* 44 (2001) 1483.
- [67] S.K. Kearsley, G.M. Smith, *Tetrahedron Comput* 3 (1990) 615.
- [68] MOE, 2008.10 of Chemical Computing Group. Inc.
- [69] T.A. Halgren, *J. Comput. Chem.* 17 (1996) 490.
- [70] W. Gerhard, S. Thomas, B. Fabian, L. Thierry, *Drug Discov. Today* 13 (2008) 23.
- [71] DSV Pro. Accelrys Software Inc., 2005.
- [72] M.B. Devani, C.J. Shishoo, U.S. Pathak, S.H. Parikh, G.F. Shah, A.C. Padhya, *J. Pharm. Sci.* 65 (1976) 660.
- [73] P. Sukumaran, *Indian J. Chem.* 28B (1989) 642.
- [74] V.J. Ram, M. Verma, *Indian J. Chem.* 31B (1992) 195.
- [75] S. Hayao, H.J. Havera, W.G. Strycker, T.J. Leipzig, *J. Med. Chem.* 10 (1967) 400.
- [76] Y. Yasuda, A. Nakada, K. Miyazaki, *Jpn. Kokai Patent* 74 36,830, 1974; *Chem. Abstr.* 83 (1975) 54567x.
- [77] M. Sharma, K. Shanker, K.P. Bhargava, M. Kishor, *Indian J. Pharm. Sci.* 1 (1979) 44.